Study of semileptonic decays $B \to \pi l^+ l^-$ and $B \to \rho l^+ l^-$ in nonuniversal Z' model

P. Nayek,[*] P. Maji, and S. Sahoo[†]

Department of Physics, National Institute of Technology Durgapur, Durgapur 713209 West Bengal, India

(Received 29 June 2018; published 28 January 2019)

Semileptonic B-meson decays induced by $b \to s(d)l^+l^-$ flavor-changing neutral current (FCNC) transitions are very important to probe the quark-flavor sector of the standard model (SM) and also offer a probe to test new physics (NP). Although there exist a lot of precise results on $b \to sl^+l^-$-induced processes, there is a lack of sufficient data for $b \to dl^+l^-$-induced decays. Here, we are interested to study $B \to \pi l^+ l^-$ and $B \to \rho l^+ l^-$ decays that proceed via a $b \to dl^+l^-$ transition at the quark level. In this work, we investigate the differential branching ratio, forward-backward asymmetry, CP violation asymmetry, and lepton polarization asymmetry in these two decay channels in a nonuniversal Z' model. We find a significant deviation from the SM value of these physical observables for these decays which provide a clear conjecture for NP arising from the Z' gauge boson.

DOI: 10.1103/PhysRevD.99.013005

I. INTRODUCTION

In recent years, a broad amount of experimental data on many observables of rare b-hadron decays have been compiled by LHCb, ATLAS, and CMS experiments at the LHC. Though we have found a puzzling list of deviations between experimental and theoretical values of flavor observables, there is no such direct evidence for a new physics (NP) effect that shows a large discrepancy from the standard model (SM). Some experimentally observed parameters that show small inconsistencies from the SM are the angular observable P_5' [1–5] of $B \to K^* \mu^+ \mu^-$ decay mode, the observation of more than 3σ deviation in the measurements of the decay rate of the $B_S \to \varphi \mu^+ \mu^-$ [6] process, the branching ratio of hadronic decays $b \to s\mu^+\mu^-$ [7–9], and the observation of lepton flavor universality (LFU) violation in $R_K = \mathscr{B}(B^+ \to K^+ \mu^+ \mu^-)/\mathscr{B}(B^+ \to K^+ e^+ e^-)$ [10] and $R_{K^*} = \mathscr{B}(B \to K^* \mu^+ \mu^-)/\mathscr{B}(B \to K^* e^+ e^-)$ [11]. These deviations explain several anomalies in rare B-meson decays particularly which are induced by the flavor-changing neutral current (FCNC) transition $b \to s(d)$. Thus, it is essential to study these anomalies in various NP models as well as in a model-independent way. Some of the NP models that can illustrate these discrepancies from the SM are the models with an extra Z' boson [12,13] and/or additional Higgs doublets [14] and the models with lepto-quarks [15–18], etc.

Rare B-meson decays which are induced by FCNC transition $b \to s(d)$ play one of the most important roles in the research area of particle physics, especially in the flavor sector of the SM. These decays occur at the loop level and generally are suppressed at the tree level in SM. On the basis of many experimental observations, it is found that the semileptonic rare B-meson decays are challenging because of small branching ratio ($\mathcal{O}(10^{-6})$ for $b \to sl^+l^-$ and $\mathcal{O}(10^{-8})$ for $b \to dl^+l^-$ transition [19,20]) and due to the presence of low p_T electrons and muons in the final state which are very problematic to reconstruct, particularly in hadronic environments. The exclusive semileptonic decays $B \to Ml^+l^-$ (M is meson) require the concept of $B \to M$ form factors in the full kinematic range $4{m_l}^2 < q^2 < (m_B - m_M)^2$. So, these semileptonic rare B-meson decay channels have received special attention [21,22]. For the semileptonic decay mode $B \to K(K^*)l^+l^-$, $B \to \pi l^+ l^-$, $B \to \rho l^+ l^-$, etc., the basic quark-level transition is $b \to s(d)l^+l^-$. Though there exist data for $b \to sl^+l^-$ processes, the detection of decays having the $b \to d$ quark-level transition is more problematic because of the lower branching ratio. For the transitions $b \to dl^+l^-$, three CKM factors which are related to the $t\bar{t}$, $c\bar{c}$, and $u\bar{u}$ loop are of the order of λ^4 i.e., $V_{tb}V_{td}^*$, $V_{cb}V_{cd}^*$, and $V_{ub}V_{ud}^* \sim \lambda^4$, where $\lambda = 0.22$. In addition, these $c\bar{c}$ and $u\bar{u}$ loop contributions are associated with different unitary phases corresponding to real intermediated states. So, we get the amplitude in such a form where different CKM phases as well as different dynamical (unitary) phases are both present. So the decays having this $b \to d$ transition have

[*]mom.nayek@gmail.com
[†]sukadevsahoo@yahoo.com

large CP violation quantities. It is also found that the leading-order contribution for $b \to d$ quark-level transition is smaller than that of the transition $b \to s$. Hence, rare semileptonic B-meson decays especially which are induced by $b \to d$ FCNC transition give a signal for NP beyond the SM. The effect of supersymmetry on some observables of $B \to \pi\tau^+\tau^-$ and $B \to \rho\tau^+\tau^-$ two decay channels are studied in [23], the decay modes $\to \pi e^+e^-$ and $B \to \rho e^+e^-$ are studied in the two Higgs doublet model [24], $B \to \pi l^+l^-$ and $B \to \rho l^+l^-(l = \tau, \mu)$ are discussed in the relativistic quark model [25], some of the angular observables for the decay mode $B \to \rho\mu^+\mu^-$ are predicted in the SM [26], and CP violation in the decay modes $\to \pi e^+e^-$ and $B \to \rho e^+e^-$ has been studied in [27]. Here, we are interested to study $B \to \pi l^+l^-$ and $B \to \rho l^+l^-$ decays in the nonuniversal Z' model.

The nonuniversal Z' model is one of the most important theoretically constructed NP models beyond the SM [28–33]. Since the Z' boson has not yet been discovered, its exact mass is unknown. But the mass of the Z' boson is constrained by direct searches from different accelerators and detectors [34–36] which give model-dependent lower bounds around 500 GeV. Sahoo *et al.* estimated the mass of the Z' boson from $B_q^0 - \overline{B_q^0}$ mixing in the range of 1352–1665 GeV [37]. If the Z' boson couples to quarks and leptons not too weakly and if its mass is not too large, it will be produced at the LHC and can be detected through its leptonic decay modes. The main discovery mode for a Z' boson at the LHC is Drell-Yan production of a dilepton resonance $pp \to Z' \to l^+l^- + X$ [38–40]. The LHC Drell-Yan data [38–40] constraints three quantities namely mass of Z' boson $(M_{Z'})$, the Z-Z' mixing angle (θ_0) and the extra U(1) effective gauge coupling (g'). At the ATLAS, the mass of the Z' boson is constrained as $M_{Z\prime} > 2.42$ TeV [38] for the sequential standard model (SSM) and $M_{Z'} > 4.1$ TeV [41] for the E_6-motivated Z'_χ. Z' bosons decaying into dilepton final states in proton-proton collisions with $\sqrt{s} = 13$ TeV have been recently studied by the CMS Collaboration [39] and predicted the lower limit on the mass of Z' boson as 4.5 TeV in the sequential standard model and 3.9 TeV in the superstring-inspired model. Using the current LHC Drell-Yan data, Bandyopadhyay *et al.* [40] have obtained $M_{Z'} > 4.4$ TeV and the Z-Z' mixing angle $\theta_0 < 10^{-3}$, when the strength of the additional U(1) gauge coupling is the same as that of the SM $SU(2)_L$. In a classically conformal $U(1)'$ extended standard model [42], an upper bound for the mass of the Z' boson is estimated as $M_{Z\prime} \leq 6$ TeV. Basically, flavor mixing between ordinary and exotic left-handed quark sector induces Z-mediated FCNC but right-handed quarks d_R, s_R and b_R have different $U(1)'$ quantum numbers which induce Z'-mediated FCNC while mixing with the exotic q_R [43–47]. The FCNC transition mediated by the addition of the Z and Z' bosons occurs at the tree level in the up-type quark sector [48]. In the Z' model, FCNC $b - s - Z'$ coupling is related to flavor diagonal couplings qqZ' and, in this similar way, the Z' boson is also coupled with leptons like llZ' [49]. The FCNC transition mediated by both the Z and Z' bosons occurs at the tree level, and this will hamper the SM contributions [46–48,50]. In this paper, we study semileptonic rare B-meson decay modes $B \to \pi l^+l^-$ and $B \to \rho l^+l^-(l = \tau, \mu, e)$ in the nonuniversal Z' model to probe the knowledge beyond the SM.

This paper is arranged as follows: In Sec. II, we present general formalism where we discuss effective Hamiltonian for $b \to dl^+l^-$ transition in SM and also define differential decay rate (DDR), forward backward (FB) asymmetry, polarization asymmetry and CP violation asymmetry briefly. In Sec. III, we discuss the decay mode $B \to \pi l^+l^-$ in the SM and define the kinematic variables associated with this decay. In Sec. IV, we discuss the decay channel $B \to \rho l^+l^-$ in the SM. In Sec. V, the contribution of the Z' gauge boson on the decay modes $B \to \pi l^+l^-$ and $B \to \rho l^+l^-$ is discussed. In Sec. VI, we present our predicted values of physical observables: differential branching ratio, FB asymmetry, polarization asymmetry, and CP violation asymmetry of $B \to \pi l^+l^-$ and $B \to \rho l^+l^-$ decays with numerical and graphical analysis. Finally, we present our conclusions in Sec. VII.

II. GENERAL FORMALISM

The semileptonic B-meson decay channels $B \to \pi l^+l^-$ and $B \to \rho l^+l^-$ involve a $b \to dl^+l^-$ quark-level transition [51]. Basically, the $b \to d$ transition involves three CKM factors i.e., $V_{tb}V_{td}^*$, $V_{cb}V_{cd}^*$, and $V_{ub}V_{ud}^*$ which are comparable in magnitude and, hence, the cross sections have significant interference terms between them. These terms introduce the possibility of observing complex CKM factors. In the SM, the effective Hamiltonian for the transition $b \to dl^+l^-$ is expressed as [51,52]

$$H_{\text{eff}} = -\frac{4G_F\alpha}{\sqrt{2}} V_{tb}V_{td}^* \left[\sum_{i=1}^{10} C_i O_i - \lambda_u \{ C_1 |O_1^u - O_1| + C_2 |O_2^u - O_2| \} \right], \tag{1}$$

where we have used the unitary condition for the CKM matrix as $V_{tb}V_{td}^* + V_{ub}V_{ud}^* \approx -V_{cb}V_{cd}^*$ and $\lambda_u = \frac{V_{ub}V_{ud}^*}{V_{tb}V_{td}^*}$. O_1 and O_2 are the current operators, $O_3 \ldots\ldots O_6$ are the QCD penguin operators, and O_9, O_{10} are two semileptonic electroweak penguin operators [51,53], G_F is the Fermi coupling constant, and C_i s are Wilson coefficients [51]. The operators $\{O_i\}$ are given in [54,55] by replacing $s \to d$. The other two operators O_1^u and O_2^u are represented as

$$O_1^u = (\bar{d}_\alpha \gamma_\mu P_L u_\beta)(\bar{u}_\beta \gamma^\mu P_L b_\alpha),$$
$$O_2^u = (\bar{d}_\alpha \gamma_\mu P_L u_\alpha)(\bar{u}_\beta \gamma^\mu P_L b_\beta), \tag{2}$$

where $P_{L,R} = (1 \mp \gamma_5)/2$. Here, we use the Wolfenstein representation of the CKM matrix with four real parameters λ, A, η, and ρ, where $\lambda = \sin\theta_C \approx 0.22$ and η is the measure of CP violation. So in terms of these parameters λ_u can be written as [23]

$$\lambda_u = \frac{\rho(1-\rho)-\eta^2}{(1-\rho)^2+\eta^2} - i\frac{\eta}{(1-\rho)^2+\eta^2} + \mathcal{O}(\lambda^2). \tag{3}$$

Now the QCD corrected matrix element can be written as

$$\mathscr{M} = \frac{G_F\alpha}{\sqrt{2}\pi} V_{tb}V_{td}^* \left\{ -2C_7^{\mathrm{eff}}\frac{m_b}{q^2}(\bar{d}i\sigma_{\mu\nu}q^\nu P_R b)(\bar{l}\gamma^\mu l) + C_9^{\mathrm{eff}}(\bar{d}\gamma_\mu P_L b)(\bar{l}\gamma^\mu l) + C_{10}(\bar{d}\gamma_\mu P_L b)(\bar{l}\gamma^\mu\gamma^5 l) \right\}. \tag{4}$$

The analytic expressions for all Wilson coefficients (except C_9^{eff} [22,52,56]) are the same as in the $b \to s$ analogue [27,51,52,55,57–61] and using the next-to-leading-order QCD correction,

$$C_7^{\mathrm{eff}} = -0.315, \qquad C_{10} = -4.642, \qquad C_9^{\mathrm{SM}} = 4.227, \tag{5}$$

and in next–to-leading approximation,

$$\begin{aligned} C_9^{\mathrm{eff}} = C_9^{\mathrm{SM}} &+ 0.124\omega(\hat{s}) + g(\hat{m}_c,\hat{s})(3C_1+C_2+3C_3 \\ &+ C_4+3C_5+C_6) + \lambda_u(g(\hat{m}_c,\hat{s}) - g(\hat{m}_u,\hat{s})) \\ &\times(3C_1+C_2) - \frac{1}{2}g(\hat{m}_d,\hat{s})(C_3+3C_4) \\ &- \frac{1}{2}g(\hat{m}_b,\hat{s})(4C_3+4C_4+3C_5+C_6) \\ &+ \frac{2}{9}(3C_3+C_4+3C_5+C_6), \end{aligned} \tag{6}$$

where $\hat{m}_q = \frac{m_q}{m_b}$. In the above equation, $\omega(\hat{s})$ represents the one-gluon correction to the matrix element of the operator O_9, and it can be represented as [62]

$$\begin{aligned} \omega(\hat{s}) = &-\frac{2}{9}\pi^2 - \frac{4}{3}Li_2(\hat{s}) - \frac{2}{3}\ln\hat{s}\ln(1-\hat{s}) \\ &- \frac{5+4\hat{s}}{3(1+2\hat{s})}\ln(1-\hat{s}) - \frac{2\hat{s}(1+\hat{s})(1-2\hat{s})}{3(1-\hat{s})^2(1+2\hat{s})}\ln\hat{s} \\ &+ \frac{5+9\hat{s}-6\hat{s}^2}{6(1-\hat{s})(1+2\hat{s})}, \end{aligned} \tag{7}$$

and the function $g(\hat{m}_q,\hat{s})$ which arises from the one-loop contributions of the four quark operators $O_1 - O_6$ is given as

$$\begin{aligned} g(\hat{m}_q,\hat{s}) = &-\frac{8}{9}\ln(\hat{m}_q) + \frac{8}{27} + \frac{4}{9}y_q - \frac{2}{9}(2+y_q)\sqrt{|1-y_q|} \\ &\times\left\{\Theta(1-y_q)\left(\ln\left(\frac{1+\sqrt{1-y_q}}{1-\sqrt{1-y_q}}\right) - i\pi\right) \right. \\ &\left. + \Theta(y_q-1)2\arctan\frac{1}{\sqrt{y_q-1}}\right\}, \end{aligned} \tag{8}$$

where $y_q \equiv \frac{4\hat{m}_q{}^2}{\hat{s}}$. $g(\hat{m}_u,\hat{s})$ and $g(\hat{m}_c,\hat{s})$ describe the effects of $u\bar{u}$ and $c\bar{c}$ loops. So with this SM value of C_9, there are two additional effective terms present in C_9^{eff}—one is due to the one-gluon correction to the matrix elements of the operator O_9 and another perturbative part arises from the one-loop contribution of the four-quark operators $O_1 - O_6$. In addition to this short distance, this C_9^{eff} also receives a long-distance contribution, which has its origin in the real $u\bar{u}$, $d\bar{d}$, and $c\bar{c}$ intermediate states i.e., the ρ, ω, J/ψ family [52]. Now, by introducing the Breit-Wigner form of the resonances prescribed in [63], C_9^{eff} can be written as

$$\begin{aligned} C_9^{\mathrm{eff}} = C_9^{\mathrm{SM}} &+ 0.124\omega(\hat{s}) + g(\hat{m}_c,\hat{s})(3C_1+C_2+3C_3+C_4+3C_5+C_6) + \lambda_u(g(\hat{m}_c,\hat{s}) - g(\hat{m}_u,\hat{s}))(3C_1+C_2) \\ &- \frac{1}{2}g(\hat{m}_d,\hat{s})(C_3+3C_4) - \frac{1}{2}g(\hat{m}_b,\hat{s})(4C_3+4C_4+3C_5+C_6) + \frac{2}{9}(3C_3+C_4+3C_5+C_6) + Y_{\mathrm{res}}, \end{aligned} \tag{9}$$

where

$$\begin{aligned} Y_{\mathrm{res}} = -\frac{3\pi}{\alpha^2}\Bigg[&\{(3C_1+C_2+3C_3+C_4+3C_5+C_6) + \lambda_u(3C_1+C_2)\} \\ &\times \sum_{V=\frac{J}{\psi},\psi',\ldots\ldots} \frac{\hat{m}_V \mathrm{Br}(V\to l^+l^-)\hat{\Gamma}^V_{\mathrm{total}}}{\hat{s}-\hat{m}_V{}^2 + i\hat{m}_V\hat{\Gamma}^V_{\mathrm{total}}} - \lambda_u g(\hat{m}_u,\hat{s})(3C_1+C_2)\times\sum_{V=\rho,\omega}\frac{\hat{m}_V \mathrm{Br}(V\to l^+l^-)\hat{\Gamma}^V_{\mathrm{total}}}{\hat{s}-\hat{m}_V{}^2 + i\hat{m}_V\hat{\Gamma}^V_{\mathrm{total}}}\Bigg], \end{aligned} \tag{10}$$

and

$$g(\hat{m}_c, \hat{s}) \to g(\hat{m}_c, \hat{s}) - \frac{3\pi}{\alpha^2} \sum_{V=\frac{J}{\psi},\psi',\ldots\ldots} \frac{\hat{m}_V \mathrm{Br}(V \to l^+l^-)\hat{\Gamma}^V_{\mathrm{total}}}{\hat{s} - \hat{m}_V{}^2 + i\hat{m}_V \hat{\Gamma}^V_{\mathrm{total}}}. \tag{11}$$

and

$$g(\hat{m}_u, \hat{s}) \to g(\hat{m}_u, \hat{s}) \left[1 - \frac{3\pi}{\alpha^2} \sum_{V=\rho,\omega} \frac{\hat{m}_V \mathrm{Br}(V \to l^+l^-)\hat{\Gamma}^V_{\mathrm{total}}}{\hat{s} - \hat{m}_V{}^2 + i\hat{m}_V \hat{\Gamma}^V_{\mathrm{total}}}\right]. \tag{12}$$

From Eq. (4) the expression of differential decay rate of the decay process $B \to Ml^+l^-$, obtained by the phase space integration is given by [23]

$$\frac{d\Gamma(B \to Ml^+l^-)}{d\hat{s}dz} = \frac{m_B}{2^9\pi^3}\lambda^{1/2}(1, \hat{s}, \hat{m}_M{}^2)\sqrt{1 - \frac{4\hat{m}_l^2}{\hat{s}}}|\mathscr{M}|^2, \tag{13}$$

where $\hat{s} = \frac{s}{m_B{}^2}$, $\hat{m}_l = \frac{m_l}{m_B}$, $\hat{m}_M = \frac{m_M}{m_B}$ are the dimensionless quantities. $\lambda(a,b,c) = a^2 + b^2 + c^2 - 2ab - 2ac - 2bc$ is the triangular function. s is the momentum transferred to the lepton pair which is the sum of the momenta of the l^+ and l^-. m_M is the mass of the meson particle M, and $z = \cos\theta$ where θ is the angle between l^- and B three momenta in the CM frame of l^+l^-. From this differential decay rate, we can define the expression of FB as [23,63]:

$$A_{\mathrm{FB}} = \frac{\int_0^1 dz \frac{d\Gamma}{d\hat{s}dz} - \int_{-1}^0 dz \frac{d\Gamma}{d\hat{s}dz}}{\int_0^1 dz \frac{d\Gamma}{d\hat{s}dz} + \int_{-1}^0 dz \frac{d\Gamma}{d\hat{s}dz}}. \tag{14}$$

To define polarization asymmetries, we first introduce the unit vectors, S in the rest frame of l^- for the polarization of lepton l^- [23,64,65] to the longitudinal direction (L), normal direction (N), and transverse direction (T).

$$\begin{aligned} S^\mu_L &\equiv (0, e_L) = \left(0, \frac{p_-}{|p_-|}\right) \\ S^\mu_N &\equiv (0, e_N) = \left(0, \frac{q \times p_-}{|q \times p_-|}\right) \\ S^\mu_T &\equiv (0, e_T) = (0, e_N \times e_L), \end{aligned} \tag{15}$$

where p_- and q are the three momenta of l^- and the photon in the CM frame of the l^+l^- system. Now boosting all three vectors in Eq. (15), the longitudinal vector becomes

$$S^\mu_L = \left(\frac{|p_-|}{m_l}, \frac{E_- p_-}{m_l |p_-|}\right), \tag{16}$$

Where the other two will remain the same. Now the expression of polarization asymmetry can be written as

$$P_x(\hat{s}) \equiv \frac{\frac{d\Gamma(S_x)}{d\hat{s}} - \frac{d\Gamma(-S_x)}{d\hat{s}}}{\frac{d\Gamma(S_x)}{d\hat{s}} + \frac{d\Gamma(-S_x)}{d\hat{s}}}, \tag{17}$$

with $x = L$, N, T, respectively, for longitudinal, normal, and transverse polarization asymmetry. We can also define CP-violating partial width asymmetry between B and $\bar{B}$ decay as

$$A_{CP} = \frac{\frac{d\Gamma}{d\hat{s}} - \frac{d\bar{\Gamma}}{d\hat{s}}}{\frac{d\Gamma}{d\hat{s}} + \frac{d\bar{\Gamma}}{d\hat{s}}}. \tag{18}$$

In the next sections, we calculate various measurable quantities that we have discussed before.

III. $B \to \pi l^+ l^-$ DECAY MODE IN THE STANDARD MODEL

In order to investigate the $B \to \pi l^+ l^-$ decay theoretically, we have to determine the decay matrix element of the weak current between the initial and final meson states. It is essential to parametrize these decay matrix elements in terms of invariant form factors. $B \to \pi l^+ l^-$ decay involves the transition between the initial B meson to scalar meson π. Using the form factors which are elaborately discussed in Appendix B [23], the decay matrix element of the weak current for the heavy to light $b \to d$ weak transition between the initial B to final π meson can be written as

$$\begin{aligned} \mathscr{M}^{B\to\pi} = \frac{G_F \alpha}{\sqrt{2}\pi} V_{tb} V^*_{td} \{ & A(p_B)_\mu (\bar{l}\gamma^\mu l) \\ & + B(p_B)_\mu (\bar{l}\gamma^\mu \gamma^5 l) + C(\bar{l}\gamma_5 l)\}, \end{aligned} \tag{19}$$

where

$$A = C_9^{\mathrm{eff}} F_1(q^2) - 2C_7^{\mathrm{eff}} \tilde{F}_T(q^2) \tag{20}$$

$$B = C_{10} F_1(q^2) \tag{21}$$

$$C = m_l C_{10} \left\{ -F_1(q^2) + \frac{m_B{}^2 - m_\pi{}^2}{q^2}(F_0(q^2) - F_1(q^2)) \right\}. \tag{22}$$

where F_1, $\tilde{F}_T$ and F_0 are summarized in Appendix B and values are given in Table X.

A. Differential decay rate (DDR)

From the above expression, we get the analytic form of the differential decay rate of the decay as

$$\frac{d\Gamma}{d\hat{s}} = \frac{G_F{}^2 m_B{}^5 \alpha^2}{3 \times 2^9 \times \pi^5} |V_{tb} V^*_{td}|^2 \lambda^{\frac{1}{2}}(1, \hat{s}, \hat{m}_\pi{}^2) \sqrt{1 - \frac{4\hat{m}_l^2}{\hat{s}}} \Sigma_\pi, \tag{23}$$

where

$$\Sigma_\pi = \lambda(1,\hat{s},\hat{m}_\pi{}^2)\left(1+\frac{2\hat{m}_l{}^2}{\hat{s}}\right)|A|^2 + \left[\lambda(1,\hat{s},\hat{m}_\pi{}^2)\left(1+\frac{2\hat{m}_l{}^2}{\hat{s}}\right)+24\hat{m}_l{}^2\right]|B|^2 + 6\frac{\hat{s}}{m_B{}^2}|C|^2 + 12\frac{\hat{m}_l}{m_B}(1+\hat{s}-\hat{m}_\pi{}^2)\mathrm{Re}(C^*B). \quad (24)$$

From Eq. (23), we can determine the expression of differential branching ratio of the decay $B\to\pi l^+l^-$.

B. CP violation

To obtain the expression of CP partial width asymmetry, first we have to write down the expression of decay rate Γ and $\bar{\Gamma}$ which is associated with the decays $\bar{B}\to\pi l^+l^-$ and $B\to\bar{\pi}l^+l^-$, respectively. Γ is obtained from Eq. (23), whereas $\bar{\Gamma}$ can be calculated from the following expression,

$$\frac{d\Gamma(B\to\bar{\pi}l^+l^-)}{d\hat{s}} = \frac{G_F{}^2 m_B{}^5\alpha^2}{3\times 2^9\times\pi^5}|V_{tb}V_{td}^*|^2\lambda^{\frac{1}{2}}(1,\hat{s},\hat{m}_\pi{}^2) \times\sqrt{1-\frac{4\hat{m}_l{}^2}{\hat{s}}}\{\Sigma_\pi + 4\mathrm{Im}\lambda_u\Delta_\pi\}, \quad (25)$$

where

$$\Delta_\pi = \left\{\mathrm{Im}(\xi_1^*\xi_2)|F_1(s)|^2 - 2C_7^{\mathrm{eff}}\mathrm{Im}\xi_2 F_T(s)F_1(s) \times\frac{m_b}{m_B+m_\pi}\right\}\lambda(1,\hat{s},\hat{m}_\pi{}^2)\left(1+\frac{2\hat{m}_l{}^2}{\hat{s}}\right), \quad (26)$$

where ξ_1 and ξ_2 can be obtained from the expression of C_9^{eff} i.e.,

$$C_9^{\mathrm{eff}} = \xi_1 + \lambda_u\xi_2. \quad (27)$$

Hence, we can obtain the expression of CP violating partial width asymmetry as

$$A_{CP}(\hat{s}) = \frac{-2\mathrm{Im}\lambda_u\Delta_\pi}{\Sigma_\pi + 2\mathrm{Im}\lambda_u\Delta_\pi}. \quad (28)$$

In this section, we have discussed two form factor dependent kinematic variables DDR and CP violating asymmetry for this decay $B\to\pi l^+l^-$ whereas FB asymmetry and polarization asymmetry are zero in the SM.

IV. $B\to\rho l^+l^-$ DECAY MODE IN STANDARD MODEL

The decay channel $B\to\rho l^+l^-$ involves the $b\to dl^+l^-$ quark-level transition. To the best of our knowledge, this decay mode has been not studied experimentally yet. The theoretical study of this decay is based on a type of effective Hamiltonian approach where the heavy degrees of freedom (e.g., gauge bosons and top quark) are integrated out [26]. This decay channel involves the transition from B meson to vector meson ρ at the hadronic level. Now the matrix element of the decay $B\to\rho l^+l^-$ in terms of form factors can be represented as follows [23]. These form factors are described broadly in Appendix C.

$$\mathscr{M}^{B\to\rho} = [i\in_{\mu\nu\alpha\beta}\epsilon^{\nu^*}p_B^\beta q^\beta A + \epsilon_\mu^* B + (\epsilon^* q)(p_B)_\mu C](\bar{l}\gamma^\mu l) + [i\in_{\mu\nu\alpha\beta}\epsilon^{\nu^*}p_B^\alpha q^\beta D + \epsilon_\mu^* E + (\epsilon^* q)(p_B)_\mu F] \times(\bar{l}\gamma^\mu l) + H(\epsilon^* q)(\bar{l}\gamma_5 l), \quad (29)$$

where

$$A = 4\frac{C_7^{\mathrm{eff}}}{s}m_b T_1(s) + C_9^{\mathrm{eff}}\frac{V(s)}{(m_B+m_\rho)} \quad (30)$$

$$B = -2\frac{C_7^{\mathrm{eff}}}{s}m_b(m_B{}^2-m_\rho{}^2)T_2(s) - \frac{1}{2}C_9^{\mathrm{eff}}(m_B+m_\rho)A_1(s) \quad (31)$$

$$C = 4\frac{C_7^{\mathrm{eff}}}{s}m_b\left\{T_2(s)+\frac{s}{(m_B{}^2-m_\rho{}^2)}T_3(\hat{s})\right\} + C_9^{\mathrm{eff}}\frac{A_2(s)}{(m_B+m_\rho)} \quad (32)$$

$$D = C_{10}\frac{V(s)}{(m_B+m_\rho)} \quad (33)$$

$$E = -\frac{1}{2}(m_B+m_\rho)A_1(s) \quad (34)$$

$$F = C_{10}\frac{A_2(s)}{(m_B+m_\rho)} \quad (35)$$

$$H = -C_{10}\frac{m_l A_2(s)}{(m_B+m_\rho)} + \frac{2m_l m_\rho}{s}(A_3(s)-A_0(s))C_{10} \quad (36)$$

where V, A_1, A_2, A_0, T_1, T_2, and T_3 are summarized in Appendix B and values are given in Table XI.

A. Differential decay rate (DDR)

Using this matrix element mentioned in Eq. (29) we can write the expression of the differential decay rate as

$$\frac{d\Gamma}{d\hat{s}} = \frac{G_F{}^2 m_B{}^5\alpha^2}{3\times 2^{10}\times\pi^5}|V_{tb}V_{td}^*|^2\lambda^{\frac{1}{2}}(1,\hat{s},\hat{m}_\rho{}^2)\sqrt{1-\frac{4\hat{m}_l{}^2}{\hat{s}}}\Sigma_\rho, \quad (37)$$

with

$$\Sigma_\rho = \left(1+\frac{2\hat{m}_l^2}{\hat{s}}\right)\lambda(1,\hat{s},\hat{m}_\rho^2)\left[4m_B^2\hat{s}|A|^2+\frac{2}{m_B^2\hat{m}_\rho^2}\left(1+12\frac{\hat{m}_\rho^2\hat{s}}{\lambda(1,\hat{s},\hat{m}_\rho^2)}|B|^2\right)\right.$$
$$\left.+\frac{m_B^2}{2\hat{m}_\rho^2}\lambda(1,\hat{s},\hat{m}_\rho^2)|C|^2+\frac{2}{\hat{m}_\rho^2}(1-\hat{m}_\rho^2+\hat{s})\mathrm{Re}(B^*C)\right]+4m_B^2\lambda(1,\hat{s},\hat{m}_\rho^2)\times(\hat{s}-4\hat{m}_l^2)|D|^2$$
$$+\frac{2}{m_B^2}\frac{[2(2\hat{m}_l^2+\hat{s})-2(2\hat{m}_l^2+\hat{s})(\hat{m}_\rho^2+\hat{s})+2\hat{m}_l^2(\hat{m}_\rho^4-26\hat{m}_\rho^2+\hat{s}^2)+\hat{s}(\hat{m}_\rho^4+10\hat{m}_\rho^2\hat{s}+\hat{s}^2)]}{\hat{m}_\rho^2\hat{s}}|E|^2$$
$$+\frac{m_B^2}{2\hat{m}_\rho^2\hat{s}}\lambda(1,\hat{s},\hat{m}_\rho^2)[(2\hat{m}_l^2+\hat{s})(\lambda(1,\hat{s},\hat{m}_\rho^2)+2\hat{s}+2\hat{m}_\rho^2)-2\{2\hat{m}_l^2\times(\hat{m}_\rho^2-5\hat{s})+\hat{s}(\hat{m}_\rho^2+\hat{s})\}]|F|^2$$
$$+3\frac{\hat{s}}{\hat{m}_\rho^2}\lambda(1,\hat{s},\hat{m}_\rho^2)|H|^2+\frac{2\lambda(1,\hat{s},\hat{m}_\rho^2)}{\hat{m}_\rho^2\hat{s}}[-2\hat{m}_l^2(\hat{m}_\rho^2-5\hat{s})+(2\hat{m}_l^2+\hat{s})-\hat{s}(\hat{m}_\rho^2+\hat{s})]\mathrm{Re}(E^*F)$$
$$+\frac{12\hat{m}_l}{m_B\hat{m}_\rho^2}\lambda(1,\hat{s},\hat{m}_\rho^2)\mathrm{Re}(H^*E)+\frac{2m_B\hat{m}_l}{\hat{m}_\rho^2}\lambda(1,\hat{s},\hat{m}_\rho^2)(1-\hat{m}_\rho^2+\hat{s})\mathrm{Re}(H^*F) \tag{38}$$

Using Eq. (37), we can calculate the differential branching ratio of this decay mode.

B. FB asymmetry

Next we discuss the FB asymmetry A_{FB} which consists of different combination of Wilson coefficients. The analysis of A_{FB} is very useful as it gives the precise information about the sign of the Wilson coefficients and the NP. In terms of form factors A_{FB} can be represented as

$$A_{\mathrm{FB}} = -\frac{12\lambda^{\frac{1}{2}}(1,\hat{s},\hat{m}_\rho^2)\sqrt{1-\frac{4\hat{m}_l^2}{\hat{s}}}\hat{s}[\mathrm{Re}(A^*D)+\mathrm{Re}(A^*E)]}{\Sigma_\rho}. \tag{39}$$

C. *CP* violation

In the similar process, the expression of the differential decay rate of $B\to\bar{\rho}l^+l^-$ can be obtained as

$$\frac{d\Gamma(B\to\bar{\rho}l^+l^-)}{d\hat{s}} = \frac{G_F^2 m_B^5\alpha^2}{3\times2^{10}\times\pi^5}|V_{tb}V_{td}^*|^2\lambda^{\frac{1}{2}}(1,\hat{s},\hat{m}_\rho^2)\sqrt{1-\frac{4\hat{m}_l^2}{\hat{s}}}(\Sigma_\rho+4\mathrm{Im}\lambda_u\Delta_\rho), \tag{40}$$

where

$$\Delta_\rho = \left[\mathrm{Im}(\xi_1^*\xi_2)\left\{4\hat{s}\frac{|V(s)|^2}{1+\hat{m}_\rho^2}+(1+\hat{m}_\rho^2)\left(\frac{6\hat{s}}{\lambda(1,\hat{s},\hat{m}_\rho^2)}+\frac{1}{2\hat{m}_\rho^2}\right)|A_1(s)|^2+\frac{\lambda(1,\hat{s},\hat{m}_\rho^2)}{2\hat{m}_\rho^2(1+m_\rho)^2}|A_2(s)|^2\right.\right.$$
$$\left.-\frac{1-\hat{m}_\rho^2-\hat{s}}{\hat{m}_\rho^2}A_1(s)A_2(s)\right\}+2\frac{C_7^{\mathrm{eff}}\hat{m}_b}{\hat{s}}\mathrm{Im}(\xi_2)\left\{8\frac{T_1(s)V(s)\hat{s}}{1+\hat{m}_\rho}+2A_1(s)T_2(s)(1+\hat{m}_\rho)^2(1-\hat{m}_\rho)\right.$$
$$\times\left(6\frac{\hat{s}}{\lambda(1,\hat{s},\hat{m}_\rho^2)}+\frac{1}{2\hat{m}_\rho^2}\right)+A_2(s)\left(T_2(s)+\frac{\hat{s}}{1-\hat{m}_\rho^2}T_3(s)\right)\frac{\lambda(1,\hat{s},\hat{m}_\rho^2)}{\hat{m}_\rho^2(1+\hat{m}_\rho)}$$
$$\left.\left.-(1+\hat{m}_\rho)A_1(s)\left(T_2(s)+\frac{\hat{s}}{1-\hat{m}_\rho^2}T_3(s)\right)\frac{1-\hat{m}_\rho^2-\hat{s}}{\hat{m}_\rho^2}+A_2(s)T_2(s)(1-\hat{m}_\rho)\frac{1-\hat{m}_\rho^2-\hat{s}}{\hat{m}_\rho^2}\right\}\right]$$
$$\times\left(1+\frac{2\hat{m}_l^2}{\hat{s}}\right)\lambda(1,\hat{s},\hat{m}_\rho^2) \tag{41}$$

Using Eqs. (37) and (40), we can calculate the decay rate of $\bar{B}\to\rho l^+l^-$ and $B\to\bar{\rho}l^+l^-$, respectively. Putting these values of decay rate, we get the expression of the partial width *CP* asymmetry as

$$A_{CP}(\hat{s}) = \frac{-2\mathrm{Im}\lambda_u\Delta_\rho}{\Sigma_\rho+2\mathrm{Im}\lambda_u\Delta_\rho}. \tag{42}$$

D. Polarization asymmetry

Along with the FB asymmetry and CP violating asymmetry we are also interested to study another form factor dependent parameter polarization asymmetry (longitudinal and normal), which is associated with the final state leptons in this decay channel. The importance of polarization asymmetry for various inclusive and exclusive semileptonic decay modes are elaborately discussed in [64–68].

1. Longitudinal polarization

The longitudinal polarization can be expressed as

$$\begin{aligned}P_L = \Bigg\{ & 24\mathrm{Re}(A^*B)(1-\hat{m}_\rho{}^2-\hat{s})\hat{s}\left(-1+\sqrt{1-\frac{4\hat{m}_l{}^2}{\hat{s}}}\right)+4m_B{}^2\lambda(1,\hat{s},\hat{m}_\rho{}^2)\hat{s}\sqrt{1-\frac{4\hat{m}_l{}^2}{\hat{s}}}\mathrm{Re}(A^*D)\\ & +\frac{1}{\hat{m}_\rho{}^2}\left(3+\sqrt{1-\frac{4\hat{m}_l{}^2}{\hat{s}}}\right)\Big[2\mathrm{Re}(B^*E)\times(1+\hat{m}_\rho{}^4+2\hat{m}_\rho{}^2\hat{s}+\hat{s}^2-2(\hat{m}_\rho{}^2+\hat{s}))+m_B{}^2\mathrm{Re}(C^*E)(1-3(\hat{m}_\rho{}^2+\hat{s})\\ & -(\hat{m}_\rho{}^2-\hat{s})^2(\hat{m}_\rho{}^2+\hat{s})+(3\hat{m}_\rho{}^4+2\hat{m}_\rho{}^2\hat{s}+3\hat{s}^2))\Big]+\frac{1}{\hat{m}_\rho{}^2}\times(\mathrm{Re}(B^*F)\times(1-\hat{m}_\rho{}^2-\hat{s})+\mathrm{Re}(C^*F)\\ & \times m_B{}^2\times\lambda(1,\hat{s},\hat{m}_\rho{}^2))\times\left[\left(3+\sqrt{1-\frac{4\hat{m}_l{}^2}{\hat{s}}}\right)\times(1+\hat{m}_\rho{}^2(\hat{m}_\rho{}^2-\hat{s})-2\hat{m}_\rho{}^2)\right.\\ & \left.+\left(3-7\sqrt{1-\frac{4\hat{m}_l{}^2}{\hat{s}}}\right)\hat{s}(\hat{m}_\rho{}^2-\hat{s})-8\hat{s}\sqrt{1-\frac{4\hat{m}_l{}^2}{\hat{s}}}\right]\Bigg\}\Big/\Sigma_\rho \end{aligned} \tag{43}$$

2. Normal polarization

Normal polarization can be represented as

$$\begin{aligned}P_N = {} & \lambda^{1/2}(1,\hat{s},\hat{m}_\rho{}^2)\sqrt{(\hat{s}-4\hat{m}_l{}^2)}\pi\left[2\mathrm{Im}(E^*F)\frac{1+\hat{m}_\rho{}^2-\hat{s}}{\hat{m}_\rho{}^2}\right.\\ & \left.+2\mathrm{Im}(A^*E+B^*D)\right].\end{aligned} \tag{44}$$

V. CONTRIBUTION OF Z′ GAUGE BOSON ON TWO DECAY MODES $B\to\pi l^+l^-$ AND $B\to\rho l^+l^-$

Theoretically, the nonuniversal Z′ boson exists in various extension of the SM by introducing extra gauge group [28,29,33]. Such models are the $SU(5)$ or E_6 model [69,70], superstring theories, and the theories with extra dimension. One fundamental feature of the Z′ model is that due to family nonuniversal couplings, the Z′ boson has flavor-changing fermionic coupling at the tree level leading to important phenomenological indications. In the nonuniversal Z′ model, FCNC transition for $b\to dl^+l^-$ process occurs at the tree level due to the presence of the nondiagonal chiral coupling matrix. The detail analysis of this model is discussed in [30]. Basically, NP effects in the nonuniversal Z′ model arise in two different ways: either by introducing new terms in Wilson coefficients or by modifying the SM structure of effective Hamiltonian. In this paper, it is desired to change two Wilson coefficients C_9^{eff} and C_{10} by considering the off-diagonal couplings of quarks as well as leptons with the Z′ boson. Here, we consider the extension of the SM by a single additional $\mathrm{U}(1)'$ gauge symmetry. In the gauge basis, the $\mathrm{U}(1)'$ currents can be written as [30,71,72]

$$J_\mu = \sum_{i,j}\bar{\psi}_i\gamma_\mu[\epsilon_{\psi_{L_{ij}}}P_L+\epsilon_{\psi_{R_{ij}}}P_R]\psi_j, \tag{45}$$

where the sum extends over all quarks, and leptons $\psi_{i,j}$ and $\epsilon_{\psi_{R,L_{ij}}}$ denote the chiral couplings of the new gauge boson. It is assumed that the Z′ couplings are diagonal but nonuniversal. Hence, flavor-changing couplings are induced by fermion mixing. FCNCs generally appear at the tree level in both the LH and RH sectors. Explicitly, we can write

$$B_{ij}^{\psi_L}\equiv(V_L^\psi\epsilon_{\psi_L}V_L^{\psi^\dagger})_{ij},\qquad B_{ij}^{\psi_R}\equiv(V_R^\psi\epsilon_{\psi_R}V_R^{\psi^\dagger})_{ij}. \tag{46}$$

The $Z'\bar{b}d$ couplings can be generated as

$$\mathcal{L}_{\mathrm{FCNC}}^{Z'} = -g'(B_{db}^L\bar{d}_L\gamma_\mu b_L+B_{db}^R\bar{d}_R\gamma_\mu b_R)Z'^\mu+\mathrm{H.c.}, \tag{47}$$

where g' is the gauge coupling associated with the $\mathrm{U}(1)'$ group, and the effective Hamiltonian can be written as

$$\begin{aligned}H_{\mathrm{eff}}^{Z'} = {} & \frac{8G_F}{\sqrt{2}}(\rho_{db}^L\bar{d}_L\gamma_\mu b_L+\rho_{db}^R\bar{d}_R\gamma_\mu b_R)\\ & \times(\rho_{ll}^L\bar{l}_L\gamma_\mu l_L+\rho_{ll}^R\bar{l}_R\gamma_\mu l_R),\end{aligned} \tag{48}$$

where

TABLE I. Numerical values of Z′ coupling parameters and weak phase [83,84].

Scenarios	$B_{db} \times 10^{-3}$	φ_{db} in Degree
S_1	0.16 ± 0.08	-33 ± 45
S_2	0.12 ± 0.03	-23 ± 21

$$\rho_{ff'}^{L,R} \equiv \frac{g' M_Z}{g M_{Z'}} B_{ff'}^{L,R}. \tag{49}$$

The current LHC Drell-Yan data [38,39] constrain the parameters: the mass of the Z′ boson $(M_{Z'})$, the Z-Z′ mixing angle (θ_0), and the extra U(1) effective gauge coupling (g') which are discussed in the Introduction. Using the current LHC Drell-Yan data, Bandyopadhyay *et al.* [40] obtained $M_{Z'} > 4.4$ TeV and the Z-Z′ mixing angle $\theta_0 < 10^{-3}$. Recently, Bobovnikov *et al.* [73] derived the constraints on the mixing angle from resonant diboson searches at the LHC at $\sqrt{s} = 13$ TeV, of the order of a few $\times 10^{-4}$. The value of $|\frac{g'}{g}|$ is undetermined [74]. However, generally one expects that $|\frac{g'}{g}| \sim 1$ if both $U(1)$ groups have the same origin from some grand unified theory and $\frac{M_z}{M_{Z'}} \sim 0.1$ for the TeV-scale Z′ [43,47]. The combined results of the four LEP experiments [75] have also proposed the existence of Z′ boson with the same couplings to fermions as that of the standard model Z boson. If $|B_{db}^L| \sim |V_{tb} V_{td}^*|$, then we get the order of $\rho_{ff'}^{L,R}$ as $\rho_{ff'}^{L,R} \sim \mathcal{O}(10^{-3})$. By neglecting $Z-Z'$ mixing and consideringthat the couplings of only the right-handed quarks with Z′ are diagonal [48,49,76–82], we can write the new modified Z′ part of the effective Hamiltonian for the transition $b \to d l^+ l^-$ as

$$H_{\rm eff}^{Z'} = \frac{2G_F}{\sqrt{2}\pi} V_{tb} V_{td}^* \left[\frac{B_{db}^L S_{ll}^L}{V_{tb} V_{td}^*} \bar{d}\gamma_\mu (1-\gamma_5) b \bar{l}\gamma^\mu (1-\gamma_5) l + \frac{B_{db}^L S_{ll}^R}{V_{tb} V_{td}^*} \bar{d}\gamma_\mu (1-\gamma_5) b \bar{l}\gamma^\mu (1+\gamma_5) l \right], \tag{50}$$

where $B_{db}^L = |B_{db}^L| e^{-i\varphi_{db}}$ indicates the off-diagonal left-handed couplings of the quark sector with the Z′ boson and φ_{db} is the new weak phase. The contributions of Z′ on the current operators, semileptonic electroweak penguin operators, and QCD penguin operators remain the same as those of the SM. In Eq. (50), the modified forms of $C_9^{\rm eff}$ and C_{10} are given. Hence, the effective Hamiltonian given in Eq. (50) can be summarized as follows,

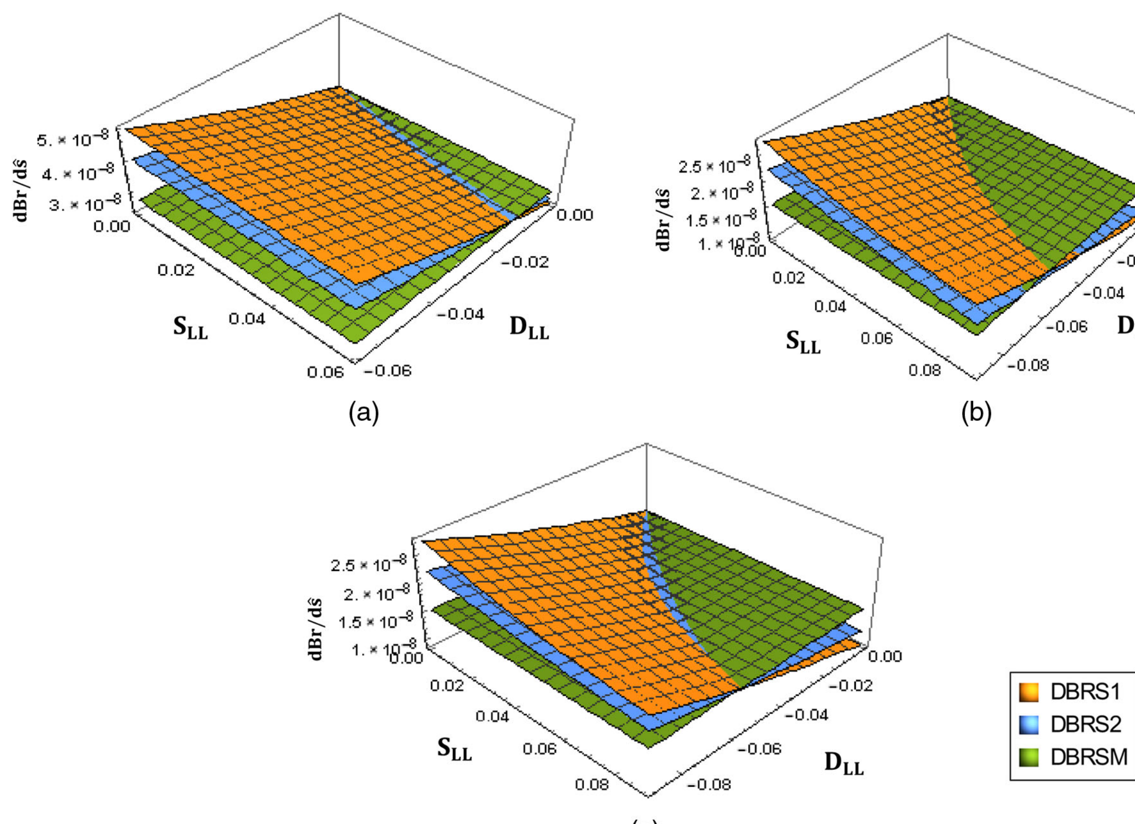

FIG. 1. The dependence of differential branching ratio $\frac{d\mathrm{Br}}{d\hat{s}}$ (DBR) on coupling parameters S_{LL} and D_{LL} for the decays (a) $B \to \pi\tau^+\tau^-$, (b) $B \to \pi\mu^+\mu^-$ and (c) $B \to \pi e^+ e^-$ for SM (DBRSM), scenario-1 (DBRS1) and scenario-2 (DBRS2).

TABLE II. Values of differential branching ratio in Z′ model for scenarios S_1 and S_2 with $S_{LL} = 0.04$ and $D_{LL} = -0.04$.

Decay mode	$DBR_{SM} \times 10^8$	$DBR_{SM+Z'} \times 10^8$	
$B \to \pi\tau^+\tau^-$	2.6 [23]	S_1	3.88
		S_2	3.451
$B \to \pi\mu^+\mu^-$	1.566	S_1	2.27
		S_2	1.634
$B \to \pi e^+e^-$	1.556	S_1	2.244
		S_2	1.621

TABLE III. Values of CP partial width asymmetry in Z′ model for scenarios S_1 and S_2 with $S_{LL} = 0.04$ and $D_{LL} = -0.04$.

Decay mode	ACP_{SM}	$ACP_{SM+Z'}$	
$B \to \pi\tau^+\tau^-$	0.0051 [23]	S_1	0.0062
		S_2	0.00608
$B \to \pi\mu^+\mu^-$	0.0059	S_1	0.0062
		S_2	0.0061
$B \to \pi e^+e^-$	0.0059	S_1	0.00629
		S_2	0.0061

$$H_{\text{eff}}^{Z'} = -\frac{4G_F}{\sqrt{2}} V_{tb}V_{td}^{*}[\wedge_{db}\, C_9^{Z'} O_9 + \wedge_{db}\, C_{10}^{Z'} O_{10}], \quad (51)$$

with

$$\wedge_{db} = \frac{4\pi e^{-i\varphi_{db}}}{\alpha V_{tb}V_{td}^{*}}, \quad (52)$$

$$C_9^{Z\prime} = |B_{db}| S_{LL}, \quad (53)$$

and

$$C_{10}^{Z'} = |B_{db}| D_{LL} \quad (54)$$

Here,

$$S_{LL} = S_{ll}^{L} + S_{ll}^{R} \quad \text{and} \quad D_{LL} = S_{ll}^{L} - S_{ll}^{R}. \quad (55)$$

S_{ll}^{L} and S_{ll}^{R} represent the couplings of the Z′ boson with the left- and right-handed leptons, respectively. In Eq. (51), the Z′ contributions of C_9^{eff} and C_{10} are given. The total contributions (SM and Z′ model) on two Wilson coefficients C_9 and C_{10} can be written as

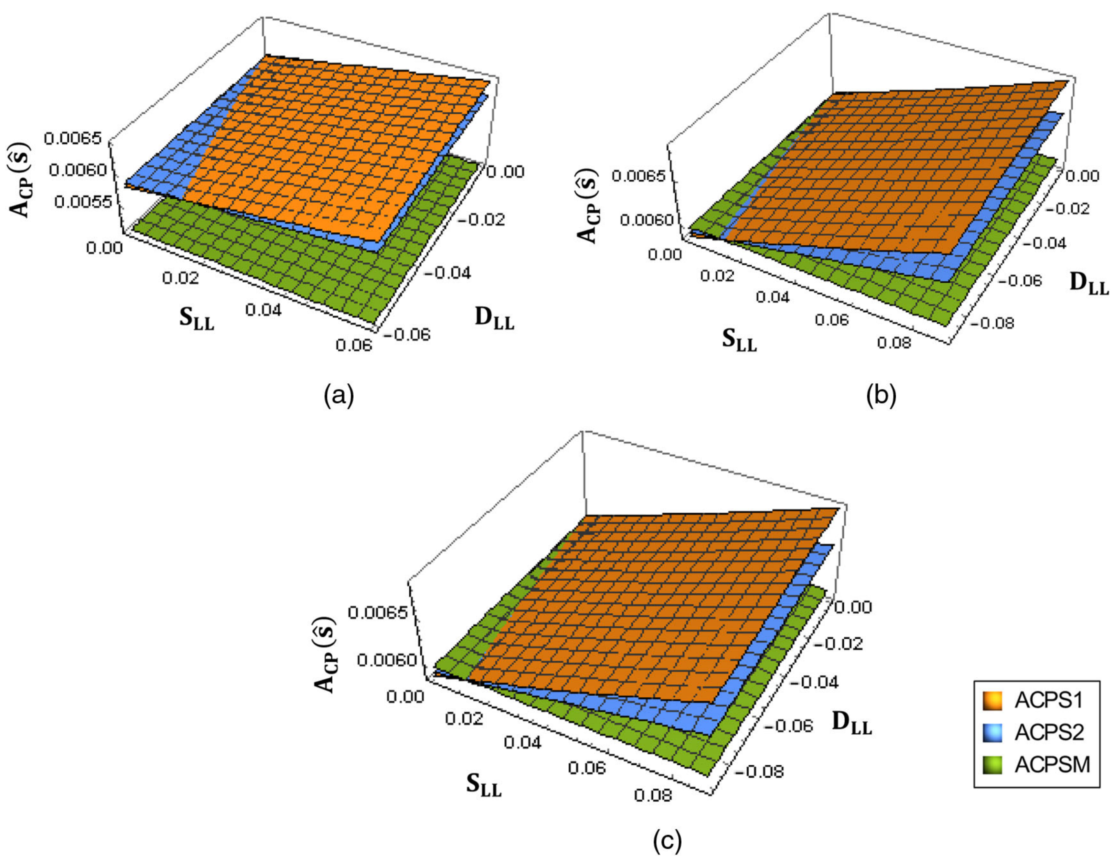

FIG. 2. The dependence of CP violation asymmetry $A_{CP}(\hat{s})$ on coupling parameters S_{LL} and D_{LL} for the decays (a) $B \to \pi\tau^+\tau^-$, (b) $B \to \pi\mu^+\mu^-$ and (c) $B \to \pi e^+e^-$ for SM (ACPSM), scenario-1 (ACPS1) and scenario-2 (ACPS2).

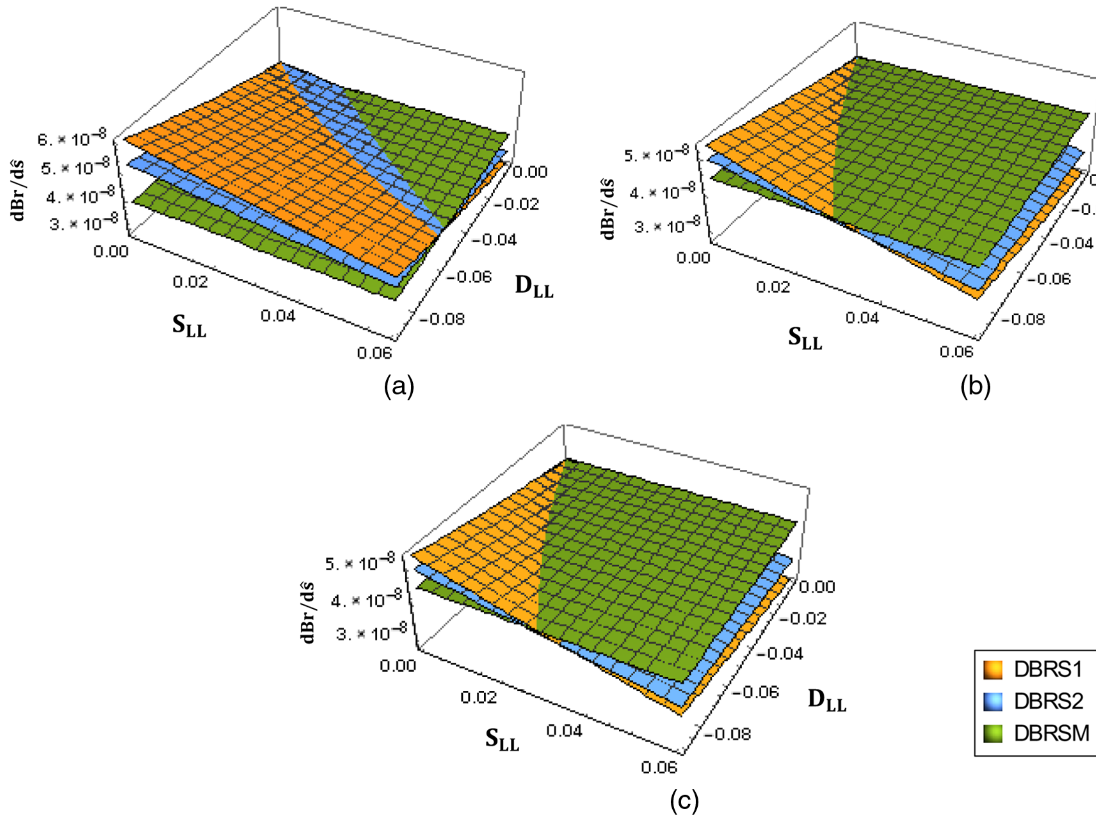

FIG. 3. The dependence of differential branching ratio $\frac{d\mathrm{Br}}{d\hat{s}}$ (DBR) on coupling parameters S_{LL} and D_{LL} for the decays (a) $B \to \rho\tau^+\tau^-$, (b) $B \to \rho\mu^+\mu^-$ and (c) $B \to \rho e^+e^-$ for SM (DBRSM), scenario-1 (DBRS1) and scenario-2 (DBRS2).

$$C_9^{\mathrm{Total}} = C_9^{\mathrm{eff}} + C_9^{\mathrm{NP}}, \tag{56}$$

$$C_{10}^{\mathrm{Total}} = C_{10} + C_{10}^{\mathrm{NP}}, \tag{57}$$

with

$$C_9^{\mathrm{NP}} = \wedge_{db}\, C_9^{Z'}, \tag{58}$$

$$C_{10}^{\mathrm{NP}} = \wedge_{db}\, C_{10}^{Z'}. \tag{59}$$

The NP contributions of the nonuniversal Z' model on the different observables: differential branching ratio, FB asymmetry, *CP* partial width asymmetry, and polarization asymmetry (longitudinal and normal) for the two decay processes $B \to \pi l^+l^-$ and $B \to \rho l^+l^-$ are analyzed in the next section.

VI. NUMERICAL ANALYSIS

In this section, we discuss DBR, FB asymmetry, *CP* asymmetry and lepton polarization asymmetry for the decay modes $B \to \pi l^+l^-$ and $B \to \rho l^+l^-$ in the frame work of the nonuniversal Z' model. To evaluate these observables in the Z' model, we have fixed the numerical values of the coupling parameter $|B_{db}|$ and the weak phase φ_{db}. But the values are strictly constrained from $\mathrm{B_d^0} - \overline{\mathrm{B_d^0}}$ mixing. These values are taken from [83,84] where NP effects to $\mathrm{B_q^0} - \overline{\mathrm{B_q^0}}(q = d, s)$ mixing in terms of coupling parameters and weak phase are discussed and encapsulated in Table I for two different scenarios S_1 and S_2. The numerical values of all input parameters shown in Table IX of Appendix A are taken from [23,85]. Putting these values in the expressions of different observables discussed in the above sections, we have shown the variations of the parameters with the coupling parameters S_{LL} and D_{LL}.

TABLE IV. Values of differential branching ratio in Z' model for scenarios S_1 and S_2 with $S_{LL} = 0.01$ and $D_{LL} = -0.09$.

Decay mode	$DBR_{SM} \times 10^8$	$DBR_{SM+Z'} \times 10^8$	
$B \to \rho\tau^+\tau^-$	3.9 [23]	S_1	5.835
		S_2	5.089
$B \to \rho\mu^+\mu^-$	4.444	S_1	5.037
		S_2	4.697
$B \to \rho e^+e^-$	4.440	S_1	5.026
		S_2	4.74

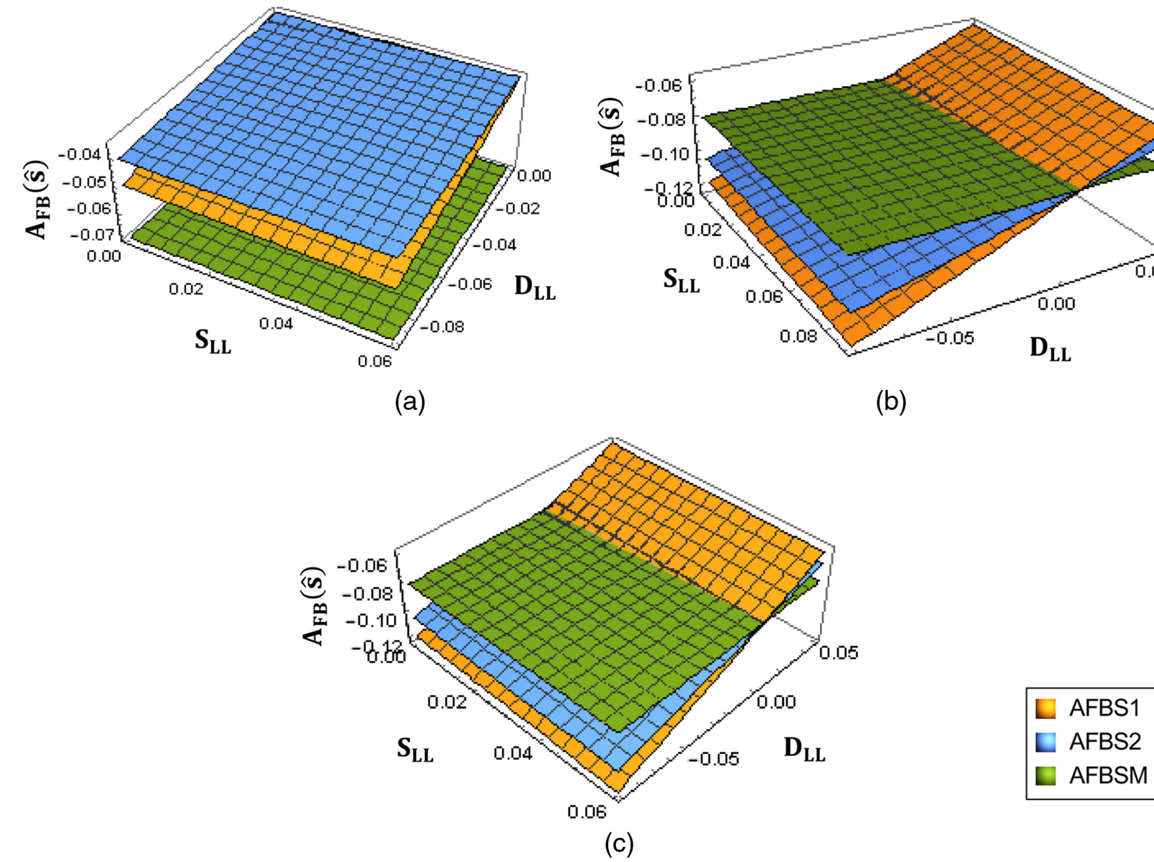

FIG. 4. The dependence of forward backward asymmetry (FB) $A_{\mathrm{FB}}(\hat{s})$ on coupling parameters S_{LL} and D_{LL} for the decays (a) $B \to \rho\tau^+\tau^-$, (b) $B \to \rho\mu^+\mu^-$ and (c) $B \to \rho e^+e^-$ for SM (AFBSM), scenario-1 (AFBS1) and scenario-2 (AFBS2).

For our calculation, we have taken the maximum values of the coupling parameter of the Z′ boson with the quark sector, i.e., B_{db}, and the new weak phase, i.e., φ_{db}, from the two scenarios given in Table I to get the maximum effect of the Z′ boson on the different physical observables of two decay modes. So we formulate two sets of scenarios of the numerical values of the coupling parameters which are as follows:

Set-I

The ranges of the coupling parameter B_{db} and weak phase φ_{db} are given in S_1. To get the magnified impact of the Z′ boson, we have taken the maximum value of these two parameters as $B_{db} = 0.24 \times 10^{-3}$ and $\varphi_{db} = 12°$

Set-II

The values of coupling parameter B_{db} vary from 0.09×10^{-3} to 0.15×10^{-3} and the weak phase φ_{db} is from $-44°$ to $-2°$ which are given in S_2. Now, we take the maximum value of these parameters as $B_{db} = 0.15 \times 10^{-3}$ and $\varphi_{db} = -2°$.

With all these numerical data, we proceed further. Considering the total contribution of Wilson coefficients C_9^{eff} and C_{10} given in Eqs. (53) and (54), we show graphically the variation of asymmetry observables for the decay modes $B \to \pi l^+l^-$ and $B \to \rho l^+l^-$ with the different values of S_{LL} and D_{LL} at a fixed value of $\hat{s}$ as 0.7. First, we represent the variations of two parameters DBR and CP partial width asymmetry for the decay $B \to \pi l^+l^-$‘ and then the variations of DBR, FB asymmetry, CP partial width asymmetry, and lepton polarization asymmetry (longitudinal and normal) for the decay $B \to \rho l^+l^-$.

From Fig. 1, we have found that for $\hat{s} = 0.7$, initially DBR slowly increases, touches the SM value at a large value of coupling parameters, and then crosses the SM value with further increase in the coupling parameters

TABLE V. Values of forward backward asymmetry in Z′ model for scenarios S_1 and S_2 with $S_{LL} = 0.02$ and $D_{LL} = -0.05$.

Decay mode	AFB_{SM}	$AFB_{SM+Z'}$	
$B \to \rho\tau^+\tau^-$	−0.072 [23]	S_1	−0.0256
		S_2	−0.0296
$B \to \rho\mu^+\mu^-$	−0.0795	S_1	−0.0575
		S_2	−0.0669
$B \to \rho e^+e^-$	−0.0797	S_1	−0.0592
		S_2	−0.0684

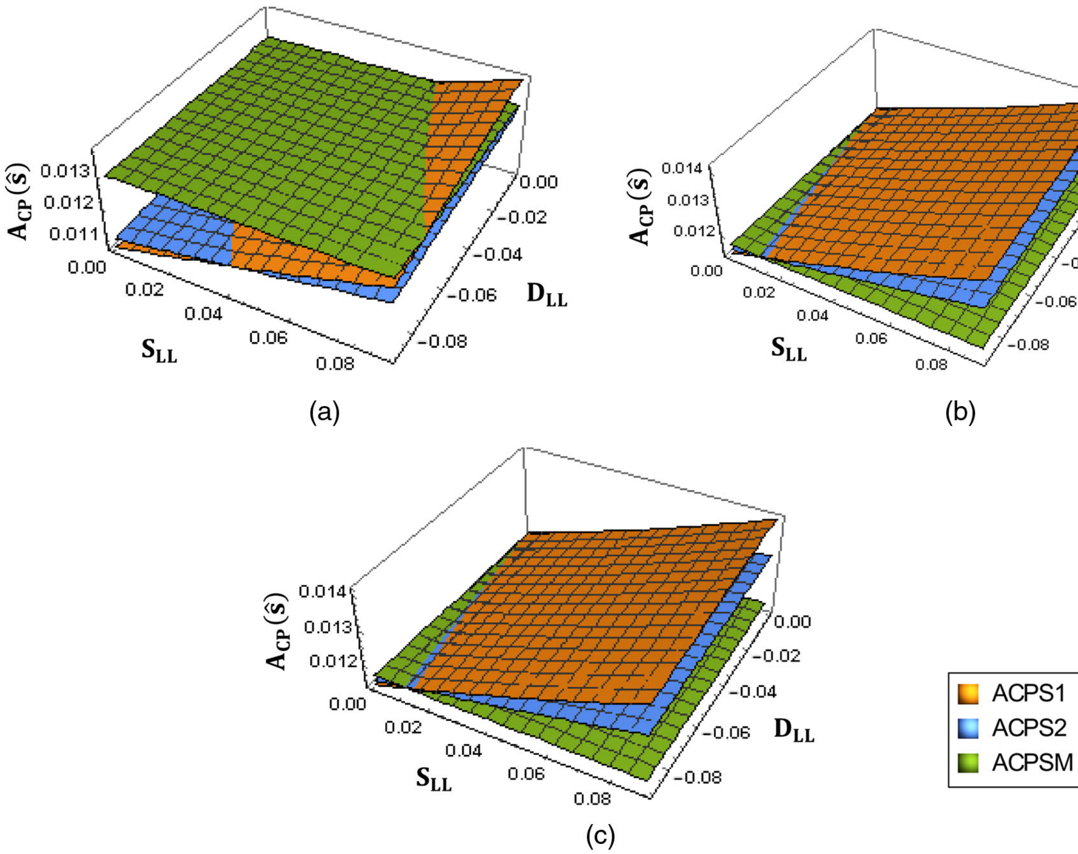

FIG. 5. The dependence of CP violation asymmetry $A_{CP}(\hat{s})$ on coupling parameters S_{LL} and D_{LL} for the decays (a) $B \to \rho\tau^+\tau^-$, (b) $B \to \rho\mu^+\mu^-$ and (c) $B \to \rho e^+e^-$ for SM (ACPSM), scenario-1 (ACPS1) and scenario-2 (ACPS2).

S_{LL} and D_{LL}. This deviation of DBR from the SM value provides a clear conjecture for NP. The values of the differential branching ratio for S_1 and S_2 with $S_{LL} = 0.04$ and $D_{LL} = -0.04$ are shown in Table II. For different values of S_{LL} and D_{LL}, the values of DBR are plotted in Fig. 1. The enhancement of DBR for the decay $B \to \pi\tau^+\tau^-$ shown in Fig. 1(a) is significantly large in comparison to the other two decays, i.e., $B \to \pi\mu^+\mu^-$ and $B \to \pi e^+e^-$, this may indicate the lepton flavor nonuniversality. Again the maximum variation of DBR for three decays $B \to \pi\tau^+\tau^-$, $B \to \pi\mu^+\mu^-$, and $B \to \pi e^+e^-$ shown in Fig. 1(a)–1(c), respectively, is observed for the S_1 scenario. Hence, we can say that with the higher contribution of the coupling parameter and weak phase, the differential branching ratio increases.

The values of CP partial width asymmetry for S_1 and S_2 with $S_{LL} = 0.04$ and $D_{LL} = -0.04$ are shown in Table III. For different values of S_{LL} and D_{LL}, the $A_{CP}(\hat{s})$ is plotted in Fig. 2. From Fig. 2, we have found that for $\hat{s} = 0.7$, initially $A_{CP}(\hat{s})$ slowly increases and crosses the SM value with increase in the coupling parameters S_{LL} and D_{LL}. This deviation of $A_{CP}(\hat{s})$ from the SM value gives a signal for NP. The enhancement of CP for the decay $B \to \pi\tau^+\tau^-$ shown in Fig. 2(a) is significantly large compared to the other two decays, i.e., $B \to \pi\mu^+\mu^-$ and $B \to \pi e^+e^-$, which points towards the lepton flavor nonuniversality.

Now we show the variations of the physical observables for the decay $B \to \rho l^+l^-$. The dependence of the differential branching ratio (DBR), forward backward asymmetry (FB), CP partial width asymmetry ($A_{CP}(\hat{s})$), and longitudinal and normal polarization asymmetry ($P_L(\hat{s})$ and $P_N(\hat{s})$) on coupling parameters for the decays $B \to \rho l^+l^-$ are represented in Figs. 3–7, respectively. For particular values of S_{LL} and D_{LL}, the values of these observables are shown in Table IV–VIII, respectively.

TABLE VI. Values of CP partial width asymmetry in Z′ model for scenarios S_1 and S_2 with $S_{LL} = 0.09$ and $D_{LL} = -0.02$.

Decay mode	ACP_{SM}	$ACP_{SM+Z'}$	
$B \to \rho\tau^+\tau^-$	0.013 [23]	S_1	0.0136
		S_2	0.0127
$B \to \rho\mu^+\mu^-$	0.0116	S_1	0.0141
		S_2	0.0130
$B \to \rho e^+e^-$	0.0116	S_1	0.0141
		S_2	0.0130

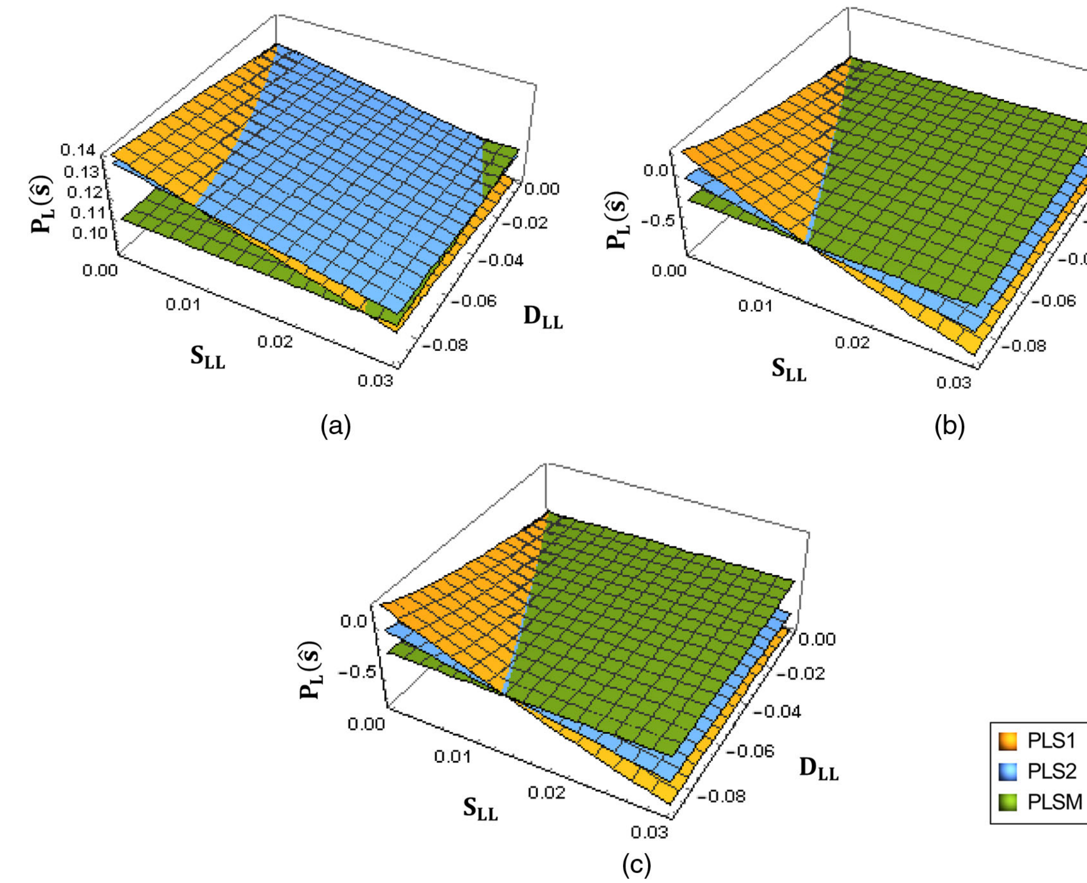

FIG. 6. The dependence of longitudinal polarization asymmetry $P_L(\hat{s})$ on coupling parameters S_{LL} and D_{LL} for the decays (a) $B \to \rho\tau^+\tau^-$, (b) $B \to \rho\mu^+\mu^-$ and (c) $B \to \rho e^+e^-$ for SM (PLSM), scenario-1 (PLS1) and scenario-2 (PLS2).

From Figs. 3(a)–3(c), similar observations [like Figs. 1(a)–1(c)] are found for the enhancement of DBR for decay modes $B \to \rho\tau^+\tau^-$, $B \to \rho\mu^+\mu^-$, and $B \to \rho e^+e^-$, respectively. Table IV shows the values of the differential branching ratio for the decay $B \to \rho\tau^+\tau^-$, $B \to \rho\mu^+\mu^-$, and $B \to \rho e^+e^-$ with $S_{LL} = 0.01$ and $D_{LL} = -0.09$.

In Fig. 4(a), we find that for $\hat{s} = 0.7$, $A_{\mathrm{FB}}(\hat{s})$ enhances significantly with the increase of coupling parameters S_{LL} and D_{LL} in $B \to \rho\tau^+\tau^-$ decay for two scenarios. But in Figs. 4(b) and 4(c), $A_{\mathrm{FB}}(\hat{s})$ increases slowly and crosses the SM value with the increase of Z′ coupling parameters for $B \to \rho\mu^+\mu^-$ and $B \to \rho e^+e^-$ decays, respectively. This deviation of $A_{\mathrm{FB}}(\hat{s})$ from the SM value provides a clue for NP. The deviation of the $B \to \rho\tau^+\tau^-$ decay is significantly large compared to $B \to \rho\mu^+\mu^-$ and $B \to \rho e^+e^-$ decays. This may indicate the lepton flavor nonuniversality. In Figs. 4(a)–4(c), we find that the variation of $A_{\mathrm{FB}}(\hat{s})$ is more for S_1 compared to S_2. Hence, we can say that with the higher value of the coupling parameter and weak phase, $A_{\mathrm{FB}}(\hat{s})$ increases. Table V shows the values of forward backward asymmetry for scenarios 1 and 2 with $S_{LL} = 0.02$ and $D_{LL} = -0.05$.

In Fig. 5(a), we find that for $\hat{s} = 0.7$, $A_{CP}(\hat{s})$ slowly increases and crosses the SM value with an increase in the coupling parameters S_{LL} and D_{LL} in $B \to \rho\tau^+\tau^-$ decay. This variation is significantly large for S_1. For S_2, $A_{CP}(\hat{s})$ touches the SM value at the higher value of coupling parameters. In Figs. 5(b) and 5(c), $A_{CP}(\hat{s})$ also increases slowly and crosses the SM value with the increase of Z′ coupling parameters for $B \to \rho\mu^+\mu^-$ and $B \to \rho e^+e^-$ decays, respectively. This deviation of $A_{CP}(\hat{s})$ from the SM value provides a clue for NP. This may indicate the lepton flavor nonuniversality due to unequal enhancement of $A_{CP}(\hat{s})$ for $B \to \rho\tau^+\tau^-$, $B \to \rho\mu^+\mu^-$ and

TABLE VII. Values of longitudinal polarization asymmetry in Z′ model for scenarios S_1 and S_2 with $S_{LL} = 0.01$ and $D_{LL} = -0.02$.

Decay mode	PL_{SM}	$PL_{SM+Z'}$	
$B \to \rho\tau^+\tau^-$	0.109 [23]	S_1	0.119
		S_2	0.124
$B \to \rho\mu^+\mu^-$	−0.26	S_1	−0.145
		S_2	0.0671
$B \to \rho e^+e^-$	−0.26	S_1	−0.145
		S_2	0.0671

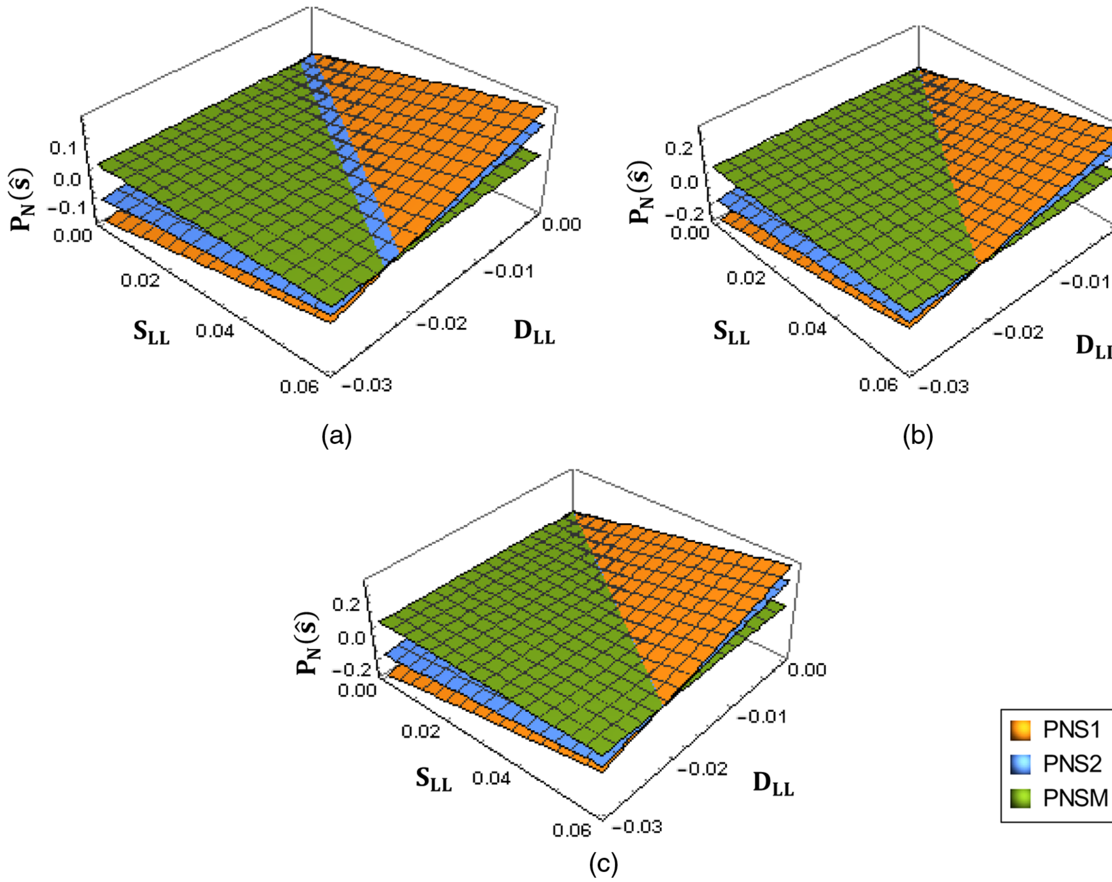

FIG. 7. The dependence of normal polarization asymmetry $P_N(\hat{s})$ on coupling parameters S_{LL} and D_{LL} for the decays (a) $B \to \rho\tau^+\tau^-$, (b) $B \to \rho\mu^+\mu^-$ and (c) $B \to \rho e^+e^-$ for SM (PNSM), scenario-1 (PNS1) and scenario-2 (PNS2).

$B \to \rho e^+e^-$ decay modes. Figs. 5(a)–(c)we find that the variation of $A_{CP}(\hat{s})$ is more for S_1 compared to S_2. Hence, we can say that with the higher value of coupling parameter and weak phase, $A_{CP}(\hat{s})$ increases. The values of CP partial width asymmetry for S_1 and S_2 from the SM value with $S_{LL} = 0.09$ and $D_{LL} = -0.02$ are shown in Table VI.

From Figs. 6, we have found that for $\hat{s} = 0.7$, initially $P_L(\hat{s})$ increases sharply and crosses the SM value with the increase in the coupling parameters S_{LL} and D_{LL}. This deviation of $P_L(\hat{s})$ from the SM value gives a signal for NP. The enhancement of $P_L(\hat{s})$ for the decay $B \to \rho\tau^+\tau^-$ shown in Fig. 6(a) is significantly large and touches the SM value at different values of coupling parameters compared to the decays $B \to \rho\mu^+\mu^-$ and $B \to \rho e^+e^-$ shown in Figs. 6(b) and 6(c), respectively. This points towards the lepton flavor nonuniversality. Again the maximum variation of $P_L(\hat{s})$ for three decays $B \to \rho\tau^+\tau^-$, $B \to \rho\mu^+\mu^-$ and $B \to \rho e^+e^-$ shown in Figs. 6(a)–6(c), respectively, is observed for S_1 scenario. Hence, we can say that with the higher value of coupling parameter and weak phase, $P_L(\hat{s})$ increases. Similar observations are also found for the normal polarization asymmetry. The variations of normal polarization asymmetry are shown in Figs. 7(a)–7(c) for the decay modes $B \to \rho\tau^+\tau^-$, $B \to \rho\mu^+\mu^-$ and $B \to \rho e^+e^-$, respectively. Tables VII and VIII show the values of the kinematic observables i.e., $P_L(\hat{s})$ and $P_N(\hat{s})$ for scenario 1 and 2 with $S_{LL} = 0.01$, $D_{LL} = -0.02$ $S_{LL} = 0.06$, $D_{LL} = -0.01$, respectively.

TABLE VIII. Values of normal polarization asymmetry in Z′ model for scenarios S_1 and S_2 with $S_{LL} = 0.06$ and $D_{LL} = -0.01$.

Decay mode	PN_{SM}	$PN_{SM+Z'}$	
$B \to \rho\tau^+\tau^-$	0.016 [23]	S_1	0.134
		S_2	0.0724
$B \to \rho\mu^+\mu^-$	0.0416	S_1	0.169
		S_2	0.031
$B \to \rho e^+e^-$	0.0416	S_1	0.170
		S_2	0.0311

VII. SUMMARY AND CONCLUSIONS

In recent years, semileptonic decays of bottom hadrons are in the focus of many theoretical and experimental studies due to increasing experimental evidence of NP. Several exclusive semileptonic decays mediated by $b \to s l^+ l^-$ have shown significant deviations from SM predictions. But it is not clear whether these deviations are due to physics beyond the SM or just hadronic artifacts [86–89]. So it is necessary to give a lot of attention to the decays mediated by the $b \to d l^+ l^-$ FCNC transition. Recently, the LHCb [90] has observed $B^+ \to \pi^+ \mu^+ \mu^-$ decay with branching ratio $\mathscr{B}(B^+ \to \pi^+ \mu^+ \mu^-) = (1.83 \pm 0.24 \pm 0.05) \times 10^{-8}$ and the CP asymmetry $A_{CP}(B^+ \to \pi^+ \mu^+ \mu^-) = (-0.11 \pm 0.12 \pm 0.01)$, where uncertainties are of a statistical and systematic nature. To the best of our knowledge, the $B \to \rho l^+ l^-$ decay has not been studied experimentally. In this paper, we have discussed several kinematic observables for $b \to d l^+ l^-$ mediated decays $B \to \pi l^+ l^-$ and $B \to \rho l^+ l^-$ in the SM and the nonuniversal Z' model. We have shown several plots of physical observables with respect to Z' coupling parameters assuming $\rho = -0.07$, $\eta = 0.34$, and $\hat{s} = 0.7$. From the significant enhancements of the parameters DBR, FB asymmetry, CP partial width asymmetry, lepton polarization asymmetry for the decay process $B \to \rho l^+ l^-$ and DBR, and CP violation asymmetry for the decay mode $B \to \pi l^+ l^-$ in the nonuniversal Z' model, we can conclude that the Z' model plays an important role in modifying the SM picture and gives signal for NP beyond the SM. Furthermore, it is found that the enhancement of the observables for the decay $B \to \pi \tau^+ \tau^-$ and $B \to \rho \tau^+ \tau^-$ is different from other decays i.e., $B \to \pi \mu^+ \mu^-$, $B \to \pi e^+ e^-$ and $B \to \rho \mu^+ \mu^-$, $B \to \rho e^+ e^-$, respectively, which may indicate the lepton flavor nonuniversality. It is expected that the measurements of these kinematic observables will provide a good hunting ground to determine the precise values of the coupling parameters of Z' boson with leptons and quarks. Furthermore, the ratio of $b \to s l^+ l^-$ and $b \to d l^+ l^-$ decays is also important to study the hypothesis of minimal flavor violation [91]. We hope the observation of $B \to \pi l^+ l^-$ and $B \to \rho l^+ l^-$ decay modes at the upcoming upgraded LHCb and/or at the Belle II detector will be very useful for searching the new physics beyond the SM.

ACKNOWLEDGMENTS

We thank the reviewers for suggesting valuable improvements to our manuscript. P. N. and S. S. would like to thank SERB, DST, Government of India, for financial support through Grant No. EMR/2015/000817. P. M. gratefully acknowledges the DST, Government of India for providing INSPIRE Fellowship (IF160115) for her research. We also acknowledge T. Bandyopadhyay, Tata Institute of Fundamental Research, Mubmai, India, for useful discussions.

APPENDIX A: INPUT PARAMETERS

TABLE IX. Numerical values of input parameters [23,85].

Parameters	Value
$m_u = m_d$	10 MeV
m_b	4.8 GeV
m_c	1.4 GeV
m_t	176 GeV
m_B	5.26 GeV
m_π	0.135 GeV
m_ρ	0.768 GeV
$\lvert V_{tb} V_{td}^* \rvert$	0.011
α	1/137
G_F	1.17×10^{-5} GeV^{-2}
m_τ	1.77 GeV
τ_B	1.54×10^{-12} s
ρ	−0.07
η	0.34

APPENDIX B: FORM FACTORS FOR THE $B \to \pi$ TRANSITION

The form factors which are used to determine the matrix element of $B \to \pi l^+ l^-$ decay process are given by Coleangelo *et al.* [92]. The matrix elements are in terms of form factors as follows [23,92]:

$$\langle \pi(p_\pi) | \bar{d} \gamma_\mu P_{L,R} b | B(p_B) \rangle = \frac{1}{2} \left\{ (2p_B - q)_\mu F_1(q^2) + \frac{{m_B}^2 - {m_\pi}^2}{q^2} q_\mu (F_0(q^2) - F_1(q^2)) \right\} \tag{B1}$$

$$\langle \pi(p_\pi) | \bar{d} i \sigma_{\mu\nu} q^\nu P_{L,R} b | B(p_B) \rangle = \frac{1}{2} \{ (2p_B - q)_\mu - ({m_B}^2 - {m_\pi}^2) q_\mu \} \frac{F_T(q^2)}{m_B + m_\pi} \tag{B2}$$

To get the matrix element for the scalar current, we have to multiply Eq. (B1) by q_μ

$$\langle \pi(p_\pi) | \bar{d} P_R b | B(p_B) \rangle = \frac{1}{2m_b} ({m_B}^2 - {m_\pi}^2) F_0(q^2). \tag{B3}$$

The definition of form factors given in Eqs. (B1)–(B3) is represented as

$$F_0(q^2) = \frac{F_0(0)}{1 - q^2/7^2}, \tag{B4}$$

TABLE X. Numerical values of form factors [23].

Form Factors	Value
$F_0(0)$	0
$F_1(0)$	0.25
$F_T(0)$	−0.14

$$F_1(q^2) = \frac{F_1(0)}{1 - q^2/5.3^2}, \tag{B5}$$

$$F_T(q^2) = \frac{F_T(0)}{(1 - q^2/7^2)(1 - q^2/5.3^2)}, \tag{B6}$$

$$\tilde{F}_T(q^2) = \frac{F_T(q^2)}{(m_B + m_\pi)} m_b, \tag{B7}$$

where q^2 is in the units of GeV^2 and the values of $F_0(0)$, $F_1(0)$, and $F_T(0)$ are encapsulated as follows.

TABLE XI. Numerical values of form factors [23].

Form facors	Value
$V(0)$	0.47
$A_1(0)$	0.37
$A_2(0)$	0.4
$A_0(0)$	0.3
$T_1(0)$	0.19
$T_2(0)$	0.19
$T_3(0)$	−0.7

APPENDIX C: FORM FACTORS FOR THE $B \to \rho$ TRANSITION

We use the form factors given by Coleangelo *et al.* [92] for the transition $B \to \rho$ [23]:

$$\langle \rho(p_\rho)|\bar{d}\gamma_\mu P_L b|\bar{B}(p_B)\rangle = i \in_{\mu\nu\alpha\beta} \epsilon^{\nu^*} p_B^\alpha q^\beta \frac{V(q^2)}{m_B + m_\rho} - \frac{1}{2}\Big\{\epsilon_\mu (m_B + m_\rho) A_1(q^2) - (\in^* q)(2p_B - q)_\mu \frac{A_1(q^2)}{m_B + m_\rho} - \frac{2m_\rho}{q^2}(\in^* q)[A_3(q^2) - A_0(q^2)]\Big\}, \tag{C1}$$

$$\langle \rho(p_\rho)|\bar{d}i\sigma_{\mu\upsilon} q^\upsilon P_{L,R} b|\bar{B}(p_B)\rangle = -2i \in_{\mu\nu\alpha\beta} \epsilon^{\nu^*} p_B^\alpha q^\beta T_1(q^2) \pm [\in_\mu^* ({m_B}^2 - {m_\rho}^2) - (\in^* q)(2p_B - q)_\mu] T_2(q^2) \pm (\in^* q)\left[q_\mu - \frac{q^2}{({m_B}^2 - {m_\rho}^2)}(2p_B - q)_\mu\right] T_3(q^2), \tag{C2}$$

where $\in$ is the polarization vector of the ρ meson. Now to get the matrix element for the scalar (pseudosacalar) current, we have to multiply both sides of Eq. (C1) by q^μ. Hence, we get

$$\langle \rho(p_\rho)|dP_R b|\bar{B}(p_B)\rangle = -\frac{m_\rho}{m_b}(\in^* q) A_0(q^2). \tag{C3}$$

In the above equations, the definitions of the form factors are represented as follows:

$$V(q^2) = \frac{V(0)}{1 - q^2/5^2}, \tag{C4}$$

$$A_1(q^2) = A_1(0)(1 - 0.023q^2), \tag{C5}$$

$$A_2(q^2) = A_2(0)(1 + 0.034q^2), \tag{C6}$$

$$A_0(q^2) = \frac{A_3(0)}{1 - q^2/4.8^2}, \tag{C7}$$

$$A_3(q^2) = \frac{m_B + m_\rho}{2m_\rho} A_1(q^2) - \frac{m_B - m_\rho}{2m_\rho} A_2(q^2), \tag{C8}$$

$$T_1(q^2) = \frac{T_1(0)}{1 - q^2/5.3^2}, \tag{C9}$$

$$T_2(q^2) = T_2(0)(1 - 0.02q^2), \tag{C10}$$

$$T_3(q^2) = T_3(0)(1 + 0.005q^2). \tag{C11}$$

The values of $V(0)$, $A_1(0)$, $A_2(0)$, $A_0(0)$, $T_1(0)$, $T_2(0)$, and $T_3(0)$ are tabulated as follows:

[1] R. Aaij *et al.* (LHCb Collaboration), J. High Energy Phys. 02 (2016) 104.
[2] S. Wehle *et al.* (Belle Collaboration), Phys. Rev. Lett. **118**, 111801 (2017).
[3] A. Abesselam *et al.* (Belle Collaboration), arXiv:1604.04042.
[4] Technical Report, ATLAS-CONF-2017-023 (CERN, Geneva, 2017), (https://cds.cern.ch/record/2258146/files/ATLAS-CONF-2017-023.pdf).
[5] R. Aaij *et al.* (LHCb Collaboration), Phys. Rev. Lett. **111**, 191801 (2013).
[6] R. Aaij *et al.* (LHCb Collaboration), J. High Energy Phys. 09 (2015) 179.
[7] R. Aaij *et al.* (LHCb Collaboration), J. High Energy Phys. 06 (2014) 133.
[8] R. Aaij *et al.* (LHCb Collaboration), J. High Energy Phys. 09 (2015) 179.
[9] V. Khachatryan *et al.* (CMS Collaboration), Phys. Lett. B **753**, 424 (2016).
[10] R. Aaij *et al.* (LHCb Collaboration), Phys. Rev. Lett. **113**, 151601 (2014).
[11] R. Aaij *et al.* (LHCb Collaboration), J. High Energy Phys. 08 (2017) 055.
[12] A. Crivellin, L. Hofer, J. Matias, U. Nierste, S. Pokorski, and J. Rosiek, Phys. Rev. D **92**, 054013 (2015).
[13] R. Gauld, F. Goertz, and U. Haisch, J. High Energy Phys. 01 (2014) 069.
[14] A. Crivellin, G. D'Ambrosio, and J. Heeck, Phys. Rev. Lett. **114**, 151801 (2015).
[15] M. Bauer and M. Neubert, Phys. Rev. Lett. **116**, 141802 (2016).
[16] S. Fajfer and N. Kosnik, Phys. Lett. B **755**, 270 (2016).
[17] S. Sahoo and R. Mohanta, Phys. Rev. D **93**, 034018 (2016).
[18] S. Sahoo and R. Mohanta, Phys. Rev. D **91**, 094019 (2015).
[19] A. Ali, Deutsches Elektronen synchrotron DESY Report No. DESY 97-192.
[20] P. Ball *et al.*, B decays, in *Proceedings of the Workshop on Standard Model Physics at the LHC, 1999*, (CERN, Geneva, switzerland, 2000).
[21] D. A. Demir, K. A. Oliev, and M. B. Voloshin, Phys. Rev. D **66**, 034015 (2002); C. Bobeth, T. Ewerth, F. Kruger, and J. Urban, Phys. Rev. D **64**, 074014 (2001); G. Erkol and G. Turan, J. High Energy Phys. 02 (2002) 015.
[22] E. O. Iltan, Int. J. Mod. Phys. A **14**, 4365 (1999); T. M. Aliev and M. Savci, Phys. Rev. D **60**, 014005 (1999).
[23] S. Rai Choudhury and N. Gaur, Phys. Rev. D **66**, 094015 (2002).
[24] T. M. Aliev and M. Savci, Phys. Rev. D **60**, 014005 (1999).
[25] R. N. Faustov and V. O. Galkin, Eur. Phys. J. C **74**, 2911 (2014).
[26] B. Kindra and N. Mahajan, Phys. Rev. D **98**, 094012 (2018).
[27] F. Krüger and L. M. Sehgal, Phys. Rev. D **56**, 5452 (1997).
[28] J. Hewett and T. Rizzo, Phys. Rep. **183**, 193 (1989).
[29] A. Leike, Phys. Rep. **317**, 143 (1999).
[30] P. Langacker and M. Plümacher, Phys. Rev. D **62**, 013006 (2000).
[31] S. Sahoo, Indian J. Phys. **80**, 191 (2006).
[32] D. Feldman, Z. Liu, and P. Nath, Phys. Rev. Lett. **97**, 021801 (2006).
[33] P. Langacker, Rev. Mod. Phys. **81**, 1199 (2009).
[34] F. Abe *et al.* (CDF Collaboration), Phys. Rev. Lett. **77**, 438 (1996).
[35] F. Abe *et al.* (CDF Collaboration), Phys. Rev. Lett. **67**, 2418 (1991).
[36] D. Abbaneo *et al.*, arXiv:hep-ex/0212036.
[37] S. Sahoo, C. K. Das, and L. Maharana, Int. J. Mod. Phys. A **26**, 3347 (2011).
[38] M. Aaboud *et al.* (ATLAS Collaboration), J. High Energy Phys. 01 (2018) 055.
[39] A. M. Sirunyan *et al.* (CMS Collaboration), J. High Energy Phys. 06 (2018) 120.
[40] T. Bandyopadhyay, G. Bhattacharyya, D. Das, and A. Raychaudhuri, Phys. Rev. D **98**, 035027 (2018).
[41] M. Aaboud *et al.* (ATLAS Collaboration), J. High Energy Phys. 10 (2017) 182.
[42] S. Oda, N. Okda, and D. Takahashi, Phys. Rev. D **92**, 015026 (2015).
[43] V. Barger, C.-W. Chiang, P. Langacker, and H. S. Lee, Phys. Lett. B **580**, 186 (2004).
[44] K. S. Babu, C. Kolda, and J. March-Russell, Phys. Rev. D **54**, 4635 (1996); **57**, 6788 (1998).
[45] S. Sahoo and L. Maharana, Phys. Rev. D **69**, 115012 (2004).
[46] V. Barger, C.-W. Chiang, P. Langacker, and H. S. Lee, Phys. Lett. B **598**, 218 (2004).
[47] V. Barger, C.-W. Chiang, J. Jiang, and P. Langacker, Phys. Lett. B **596**, 229 (2004).
[48] A. Arhrib, K. Chung, C.-W. Chiang, and T.-C. Yuan, Phys. Rev. D **73**, 075015 (2006).
[49] K. Cheung, C.-W. Chiang, N. G. Deshpande, and J. Jiang, Phys. Lett. B **652**, 285 (2007).
[50] Y. Nir and D. Silverman, Phys. Rev. D **42**, 1477 (1990).
[51] G. Buchalla, A. Buras, and M. Lautenbacher, Rev. Mod. Phys. **68**, 1125 (1996).
[52] F. Krüger and L. M. Sehgal, Phys. Rev. D **55**, 2799 (1997); T. M. Aliev, V. Bashing, and M. Savei, Eur. Phys. J. C **31**, 511 (2003).
[53] A. Ali, arXiv:hep-ph/9709507.
[54] B. Grinstein, M. J. Savage, and M. B. Wise, Nucl. Phys. **B319**, 271 (1989).
[55] M. Misiak, Nucl. Phys. **B393**, 23 (1993).
[56] S. Rai Choudhury, Phys. Rev. D **56**, 6028 (1997).
[57] A. J. Buras and M. Münz, Phys. Rev. D **52**, 186 (1995).
[58] G. Cella, G. Ricciardi, and A. Viceré, Phys. Lett. B **258**, 212 (1991).
[59] Z. Xiong and J. M. Yang, Nucl. Phys. **B628**, 193 (2002); C. Bobeth, A. J. Buras, F. Krüger, and J. Urban, Nucl. Phys. **B630**, 87 (2002); C. Huang, W. Liao, and Q. Yan, Phys. Rev. D **59**, 011701 (1998).
[60] P. L. Cho, M. Misiak, and D. Wyler, Phys. Rev. D **54**, 3329 (1996); J. L. Hewett and J. D. Wells, Phys. Rev. D **55**, 5549 (1997).
[61] B. Grinstein, M. J. Savage, and M. B. Wise, Nucl. Phys. **B319**, 271 (1989).
[62] M. Jezabek and J. H. Kühn, Nucl. Phys. **B320**, 20 (1989).
[63] A. Ali, T. Mannel, and T. Morozumi, Phys. Lett. B **273**, 505 (1991); C. S. Lim, T. Morozumi, and A. I. Sanda, Phys. Lett. B **218**, 343 (1989); N. G. Deshpande, J. Trampetic, and K. Panose, Phys. Rev. D **39**, 1461 (1989); P. J. O'Donnell and H. K. Tung, Phys. Rev. D **43**, R2067 (1991).

[64] S. Rai Choudhury, A. Gupta, and N. Gaur, Phys. Rev. D **60**, 115004 (1999); S. Rai. Choudhury, N. Gaur, and A. Gupta, Phys. Lett. B **482**, 383 (2000).

[65] F. Krüger and L. M. Sehgal, Phys. Lett. B **380**, 199 (1996); J. L. Hewett, Phys. Rev. D **53**, 4964 (1996).

[66] S. Rai Choudhury, N. Gaur, and N. Mahajan, Phys. Rev. D **66**, 054003 (2002); S. Rai Choudhury and N. Gaur, arXiv: hep-ph/0205076.

[67] S. Fukae, C. S. Kim, and T. Yoshikawa, Phys. Rev. D **61**, 074015 (2000).

[68] T. M. Aliev, M. K. Cakmak, and M. Savci, Nucl. Phys. **B607**, 305 (2001); T. M. Aliev, M. K. Cakmak, A. Ozpineci, and M. Savci, Phys. Rev. D **64**, 055007 (2001).

[69] V. Barger, M. S. Berger, and R. J. N. Phillips, Phys. Rev. D **52**, 1663 (1995).

[70] J. Bernabeu, E. Nardi, and D. Tommasini, Nucl. Phys. **B409**, 69 (1993).

[71] L. V. Barger, L. L. Everett, J. Jiang, P. Langacker, T. Liu, and C. E. M. Wagner, J. High Energy Phys. 12 (2009) 048.

[72] C.-W. Chiang, L. R. Hui, and L. C. Dian, Chin. Phys. C **36**, 14 (2012).

[73] I. D. Bobovnikov, P. Osland, and A. A. Pankov, arXiv: 1809.08933.

[74] M. Cvetic and B. W. Lynn, Phys. Rev. D **35**, 51 (1987).

[75] S. Schael *et al.* (LEP Electroweak Working Group), Phys. Rep. **532**, 119 (2013).

[76] Q. Chang and Y.-H. Gao, Nucl. Phys. B, Proc. Suppl. **115**, 263 (2003).

[77] Y. Li and J. Hua, Eur. Phys. J. C **71**, 1775 (2011).

[78] H. Chen and H. Hatanaka, Phys. Rev. D **73**, 075003 (2006).

[79] W. Chiang, N. G. Deshpande, and J. Jiang, J. High Energy Phys. 08 (2006) 075.

[80] V. Bargar, L. Everett, J. Jiang, P. Langacker, T. Liu, and C. E. M. Wagner, Phys. Rev. D **80**, 055008 (2009).

[81] R. Mohanta and A. K. Giri, Phys. Rev. D **79**, 057902 (2009).

[82] J. Hua, C. S. Kim, and Y. Li, Eur. Phys. J. C **69**, 139 (2010).

[83] Q. Chang, X. Q. Li, and Y. D. Yang, J. High Energy Phys. 02 (2010) 082.

[84] Q. Chang and Y. D. Yang, Nucl. Phys. **B852**, 539 (2011).

[85] C. Patrignani *et al.* (Particle Data Group), Chin. Phys. C **40**, 100001 (2016).

[86] J. Lyon and R. Zwicky, arXiv:1406.0566.

[87] S. Jäger and J. Martin Camalich, J. High Energy Phys. 05 (2013) 043.

[88] M. Ciuchini, M. Fedele, E. Franco, S. Mishima, A. Paul, L. Silvestrini, and M. Valli, J. High Energy Phys. 06 (2016) 116.

[89] V. G. Chobanova, T. Hurth, F. Mahmoudi, D. Martinez Santos, and S. Neshantpour, J. High Energy Phys. 07 (2017) 025.

[90] R. Aaij *et al.* (LHCb Collaboration), J. High Energy Phys. 10 (2015) 034.

[91] G. D' Ambrosio, G. F. Giudice, G. Isidori, and A. Strumia, Nucl. Phys. **B645**, 155 (2002).

[92] P. Coleangelo, F. De. Fazio, P. Santorelli, and E. Scrimieri, Phys. Rev. D **53**, 3672 (1996).